THE JOURNAL OF BIOLOGICAL CHEMISTRY
Vol. 280, No. 26, Issue of July 1, pp. 24775–24783, 2005
Printed in U.S.A.

Membrane-proximal α/β Stalk Interactions Differentially Regulate Integrin Activation*

Received for publication, August 19, 2004, and in revised form, April 21, 2005
Published, JBC Papers in Press, April 29, 2005, DOI 10.1074/jbc.M409548200

Tetsuji Kamata‡§, Makoto Handa¶, Yukiko Sato‡, Yasuo Ikeda‖, and Sadakazu Aiso‡

From the Departments of ‡Anatomy, ¶Transfusion Medicine and Cell Therapy, and ‖Internal Medicine, Keio University School of Medicine, Tokyo 160-8582, Japan

The affinity of integrin-ligand interaction is regulated extracellularly by divalent cations and intracellularly by inside-out signaling. We report here that the extracellular, membrane-proximal α/β stalk interactions not only regulate cation-induced integrin activation but also play critical roles in propagating inside-out signaling. Two closely related integrins, αIIbβ3 and αVβ3, share high structural homology and bind to similar ligands in an RGD-dependent manner. Despite these structural and functional similarities, they exhibit distinct responses to Mn^{2+}. Although αVβ3 showed robust ligand binding in the presence of Mn^{2+}, αIIbβ3 showed a limited increase but failed to achieve full activation. Swapping α stalk regions between αIIb and αV revealed that the α stalk, but not the ligand-binding head region, was responsible for the difference. A series of αIIb/αV domain-swapping chimeras were constructed to identify the responsible domain. Surprisingly, the minimum component required to render αIIbβ3 susceptible to Mn^{2+} activation was the αV calf-2 domain, which does not contain any divalent cation-binding sites. The calf-2 domain makes interface with β epidermal growth factor 4 and β tail domain in three-dimensional structure. The effect of calf-2 domain swapping was partially reproduced by mutating the specific amino acid residues in the calf-2/epidermal growth factor 4-β tail domain interface. When this interface was constrained by an artificially introduced disulfide bridge, the Mn^{2+}-induced αVβ3-fibrinogen interaction was significantly impaired. Notably, a similar disulfide bridge completely abrogated fibrinogen binding to αIIbβ3 when αIIbβ3 was activated by cytoplasmic tail truncation to mimic inside-out signaling. Thus, disruption/formation of the membrane-proximal α/β stalk interface may act as an on/off switch that triggers integrin-mediated bidirectional signaling.

Integrins are a family of α/β heterodimeric transmembrane cell surface receptors that mediate cell-extracellular matrix and cell-cell interactions. The hallmark of integrin-dependent adhesive interaction is its regulation by intracellular signaling events (inside-out signaling) and by divalent cations. In addition to mediating adhesive interactions, liganded integrins initiate signals inside the cell to modify cell behavior (outside-in signaling) and thus play fundamental roles in numerous biological processes such as differentiation, cell survival, apoptosis, and cell motility (1). Integrin-mediated bidirectional signaling is accompanied by conformational change of the integrin structure. The crystal structure of αVβ3 extracellular domains revealed an unexpected bent conformer distinct from the extended conformer observed under electron microscope (2, 3). High-resolution electron microscopic observation on truncated recombinant αVβ3 has confirmed the presence of both conformers, suggesting that the transition from one conformer to another might take place under physiological conditions (4). However, integrin extension *per se* is not required for the activation, but the swing-out of the β hybrid domain (the transition from "closed" headpiece to "open" headpiece) that accompanies the extension is the critical event (5). Thus, integrin extracellular domains undergo extensive structural rearrangement (so-called "switchblade-like" movement) upon Mn^{2+}/ligand binding. In support, fluorescence resonance energy transfer measurements between α4β1-bound peptide ligand and plasma membrane revealed that such movement actually takes place in living cells (6, 7).

Divalent cations differentially regulate integrin-ligand interaction. Whereas Mn^{2+} and, to a lesser extent, Mg^{2+} have an enhancing effect, Ca^{2+} typically has an inhibitory effect on ligand binding. Biochemical studies have suggested the existence of three classes of cation-binding sites with distinct function and preference for cations (8). The αVβ3 extracellular domains turned out to contain eight cation-binding sites. Five of them are located in the β-propeller and at the junction between the thigh and calf-1 domains of the α subunit. The other three are located in the βA domain of the β subunit. Besides the metal ion-dependent adhesion site (MIDAS), which is essential for ligand binding (9, 10), the βA domain possesses two additional sites designated ADMIDAS (adjacent to MIDAS) and LIMBS (ligand-associated metal binding site), respectively (11). Whereas ADMIDAS is occupied by a cation regardless of the presence of bound ligand, MIDAS and LIMBS have been shown to bind Mn^{2+} only in the presence of bound ligand (3, 11). A recent report by Chen *et al.* (12) suggests that the ADMIDAS is the negative regulatory site for Ca^{2+}, whereas LIMBS is the positive regulatory site for Ca^{2+}. These reports implicate that the cation-binding sites in the βA domain represent the three classes of cation-binding sites described by Mould *et al.* (8), thus they are primarily responsible for integrin affinity regulation by divalent cations. In contrast, the role of the α subunit, particularly the five cation-binding sites, has not been clearly defined.

* This work was supported by a health and labor science research grant for research on regulatory science of pharmaceuticals and medical devices from the Ministry of Health, Labor and Welfare; a grant for leading project for biosimulation from the Ministry of Education, Culture, Sports, Science and Technology; a grant from Keio Gijuku Fukuzawa Memorial Fund for the advancement of education and research (to T. K. and M. H.); a grant-in-aid for scientific research (B); a grant-in-aid for COE research; and a national grant-in-aid for the establishment of high-tech research center in a private university (to S. A.). The costs of publication of this article were defrayed in part by the payment of page charges. This article must therefore be hereby marked "*advertisement*" in accordance with 18 U.S.C. Section 1734 solely to indicate this fact.

§ To whom correspondence should be addressed: Dept. of Anatomy 3S1, Keio University School of Medicine, 35 Shinanomachi, Shinjuku-ku, Tokyo 160-8582, Japan. Tel.: 81-3-3353-1211 (ext. 63571); Fax: 81-3-5360-1524; E-mail: kamata@sc.itc.keio.ac.jp.

Two β3 integrins, αIIbβ3 and αVβ3 ,share high structural homology (13). Both integrins share a common β3 subunit and bind fibrinogen (Fbg),[1] von Willebrand factor, fibronectin, and vitronectin in an RGD-dependent manner. Despite these structural and functional similarities, divalent cations regulate ligand binding differently in these integrins. Kinetic studies have shown that Mn^{2+} supports Fbg binding to both αIIbβ3 and αVβ3, albeit with a relatively slow association rate, whereas Ca^{2+} supports Fbg binding only to αIIbβ3, but not to αVβ3 (14). In agreement, real-time measurements of Fbg binding interaction have shown that Mn^{2+} increased the affinity for Fbg in both integrins by increasing the association rate (4, 15). Consistent with these observations, αVβ3-mediated cell attachment to immobilized Fbg was greatly enhanced by Mn^{2+} but not by Ca^{2+} (14). In contrast, intact αIIbβ3 expressed on the cell surface exhibits different characteristics. First of all, cations including Mn^{2+} are unable to initiate platelet aggregation or induce Fbg binding to platelets, unless platelets are stimulated by agonists. The agonist-stimulated platelet aggregation is also poorly supported by Mn^{2+} (14, 16, 17). These lines of evidence suggest that cation-binding sites in the βA domain do not account for the distinct response to Mn^{2+} in β3 integrins, but rather that the structural difference in the α subunit may be responsible. In this study, we sought to determine the mechanism that regulates Mn^{2+}-induced activation in β3 integrins. We provide evidence that the calf-2 domain, but not the cation-binding sites, in the α subunit plays a critical role in regulating the Mn^{2+}-induced integrin activation. Furthermore, the results suggest that disruption/formation of the membrane-proximal calf-2/epidermal growth factor (EGF)4-β tail domain (βTD) interface may act as an on/off switch that propagates the conformational signals in integrin-mediated bidirectional signaling.

EXPERIMENTAL PROCEDURES

Antibodies and Reagents—Anti-αIIb monoclonal antibody (mAb) PL98DF6 (18) was a generous gift from Drs. J. Ylänne (University of Uppsala, Uppsala, Sweden) and I. Virtanen (University of Helsinki, Helsinki, Finland). Conformation-dependent anti-β3 mAbs anti-LIBS1 and anti-LIBS2 (19) were generous gifts from Dr. Mark H. Ginsberg (University of California, San Diego, CA). Anti-αIIbβ3 complex-specific ligand-mimetic mAb OP-G2 (20) was a kind gift from Dr. Yoshiaki Tomiyama (University of Osaka, Osaka, Japan). The αIIbβ3 complex-specific anti-αIIb mAb P2, anti-β3 mAb SZ21, and anti-αV mAb AMF-7 were purchased from Beckman Coulter (Fullerton, CA). Anti-αIIbβ3 complex-specific activating mAb PT25-2 and non-functional anti-β3 mAb VNR5-2 have been characterized previously (21). Fluorescein isothiocyanate (FITC)- and R-phycoerythrin-conjugated goat anti-mouse polyclonal antibodies were purchased from BIOSOURCE. Synthetic peptide Gly-Arg-Gly-Asp-Ser (GRGDS) was purchased from Peptide Research Institute (Osaka, Japan). FITC was purchased from Sigma-Aldrich. Human Fbg was purchased from Experimental Cell Research (South Bend, IN).

Construction of Mutant αIIb, αV, and β3 cDNA Clones—The full-length cDNAs for integrin αIIb, αV, and β3 subunits (generous gifts from Dr. Joseph C. Loftus, Mayor Clinic, AZ) were cloned into mammalian expression vector pBJ-1 (kindly provided by Dr. Mark Davis, University of California, San Francisco, CA). A SacI site was engineered into the αV cDNA at site homologous to the endogenous SacI site in the αIIb cDNA by site-directed mutagenesis using Transformer Site-Directed Mutagenesis Kit (BD Biosciences). The cDNAs for B/V and V/B chimeras were created by replacing the SacI-BamHI fragment between αIIb and αV. The cDNAs for αIIb/αV domain-swapping chimeras TC1C2, TC1, T, C1, C2, D, C1C2D, TC2D, and TC1D were created using the overlap extension PCR method. The domain boundaries for each chimera were set as shown in Fig. 1*A*. The cDNAs for B/V 753–755, B/V 760–764, B/V 774, B/V 781–783, B/V 787, B/V 899–900, B/V 902–904, and B/V 958–960 mutants were created by site-directed mutagenesis. In these αIIb mutants, the amino acid sequences in each of the indicated regions were replaced by the corresponding αV sequences (^{753}NSF to VSS, ^{760}VVAAE to FLPIP, Asp^{774} to Glu, ^{781}EHT to QHI, His^{787} to Arg, ^{899}QR to KS, ^{902}MTV to ILY, and ^{958}ALE to GIQ, respectively). Likewise, B/V 760, B/V 761, B/V 762, B/V 763, B/V 764, B/V 899, and B/V 900 mutants represent V760F, V761L, A762P, A763I, E764P, Q899K, and R900S mutations, respectively. The cDNAs for B/V 787/899–900 and B/V 787/900 were created from cDNAs for B/V 787 and B/V 899–900 and for B/V 787 and B/V 900, respectively, by replacing the BamHI fragment. The cDNA for B/V 760–764/787/899–900 was created from cDNAs for B/V 760–764 and B/V 787/899–900 by replacing the SacI fragment. The αV D599A, αV E636A, αV S749C, αIIb F755C, β3 D606C, β3 L717tr (β3tr), and αIIb G991tr (αIIbtr) mutants were created by site-directed mutagenesis. The β3 D606C/L717tr double mutant (606tr) was created from β3 D606C and β3 L717tr by replacing the ApaI fragment. The αIIb F755C/G991tr double mutant (755tr) was created from αIIb F755C and αIIb G991tr by replacing the BamHI fragment. The authenticity of the constructs was confirmed by DNA sequencing.

Cell Culture and Transfection—Chinese hamster ovary (CHO)-K1 cells were cultured in Dulbecco's modified Eagle's medium (Invitrogen) supplemented with 10% fetal calf serum (BIOSOURCE), 1% penicillin and streptomycin (Invitrogen), and 1% non-essential amino acids (Sigma-Aldrich) and maintained at 37 °C in a humidified incubator supplemented with 5% CO_2. Fifty μg of αV or αIIb cDNA construct was co-transfected with 50 μg of β3 cDNA construct into CHO-K1 cells by electroporation. After 48 h, the cells were detached and used for assays.

Flow Cytometry—Cells were detached with phosphate-buffered saline containing 3.5 mM EDTA. After washing, cells were incubated with mAbs in modified HEPES-Tyrode buffer (5 mM HEPES, 5 mM glucose, 0.2 mg/ml bovine serum albumin, and 1× Tyrode's solution) supplemented with 1 mM $CaCl_2$ and 1 mM $MgCl_2$ for 30 min at 4 °C. For some experiments, 1 mM GRGDS peptide was included together with mAbs. After washing, cells were incubated with R-phycoerythrin-conjugated $F(ab')_2$ fragment of goat anti-mouse IgG for 30 min at 4 °C. After washing, cells were resuspended in HEPES-buffered saline (10 mM HEPES, 150 mM NaCl, pH 7.4) containing 1 mM $CaCl_2$ and 1 mM $MgCl_2$, and fluorescence was measured on FACSCalibur (BD Biosciences). To compare the binding of conformation-dependent mAbs among cells expressing different αVβ3 mutants, each mAb binding was normalized by the expression of αVβ3. This relative mAb binding was calculated by dividing the mean fluorescent intensity obtained with each anti-LIBS mAb by the mean fluorescent intensity with non-conformation-dependent anti-β3 mAb SZ21.

Fibrinogen Binding Assay—FITC labeling of human Fbg was performed as previously described (22). Briefly, after adjusting the pH of human Fbg at 1 mg/ml in phosphate-buffered saline to 8.5 with 5% Na_2CO_3, 0.01 volume of 10 mg/ml FITC in Me_2SO was added and incubated at room temperature for 10 min. FITC-labeled Fbg was separated from free FITC on a PD-10 column (Amersham Biosciences) equilibrated with HEPES-buffered saline. The concentration and fluorescence/protein ratio of FITC-labeled Fbg was calculated as previously described. Forty-eight h after transfection, cells were detached and incubated with non-functional anti-β3 mAb VNR5-2 followed by a R-phycoerythrin-conjugated $F(ab')_2$ fragment of goat anti-mouse IgG. In some experiments, cells were treated with 10 mM dithiothreitol (DTT) prior to incubation with mAbs as described previously (21). After washing, cells were incubated with FITC-labeled Fbg (200 μg/ml) with or without 1 mM GRGDS peptide in modified HEPES-Tyrode buffer containing 1 mM $CaCl_2$ and 1 mM $MgCl_2$ or 1 mM $MnCl_2$ for 1 h at 4 °C. In some experiments, mAb PT25-2 was included at 10 μg/ml to activate αIIbβ3. After washing, fluorescence was measured on FACSCalibur. The mean Fbg binding (mean fluorescence intensity in FL1 channel) to cell populations expressing high β3 (fluorescence intensity in FL2 channel > 500) was calculated. Background binding in the presence of 1 mM GRGDS peptide was subtracted to obtain specific binding.

RESULTS

Swapping α Stalk Region Switches the Enhancing Effect of Mn^{2+} on Ligand Binding—To locate the structure in the α subunit responsible for the difference in Mn^{2+} activation, we first swapped the C-terminal stalk region consisting of the thigh, calf-1, calf-2, transmembrane (TM), and cytoplasmic domains between αIIb and αV. The B/V chimera has αIIb β-propeller joined with αV stalk, whereas the V/B chimera has

[1] The abbreviations used are: Fbg, fibrinogen; EGF, epidermal growth factor; mAb, monoclonal antibody; FITC, fluorescein isothiocyanate; DTT, dithiothreitol; TM, transmembrane; βTD, β tail domain; CHO, Chinese hamster ovary.

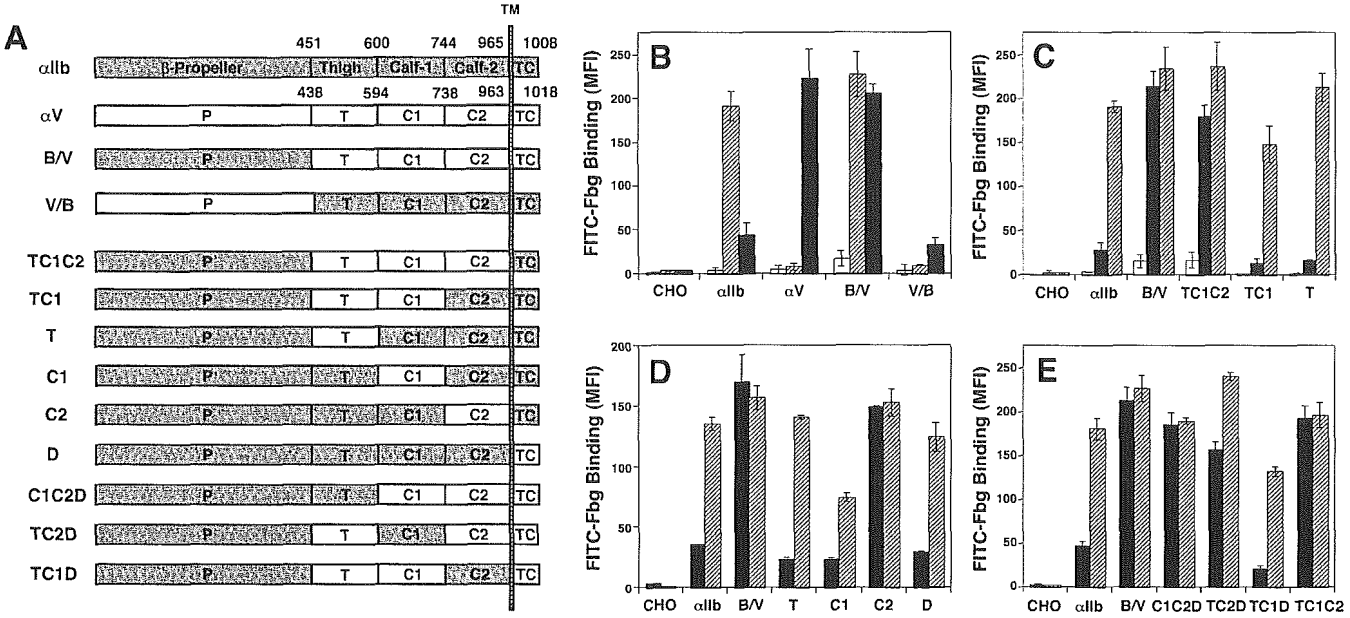

FIG. 1. **The calf-2 domain in integrin α subunit regulates Mn^{2+}-induced integrin activation.** *A*, schematic representation of the αIIb/αV chimeras. Positions of the domain boundaries are indicated. The specific binding of FITC-Fbg is presented in mean fluorescent intensity. *B*, FITC-Fbg binding to cells expressing α stalk-swapping chimeras (B/V and V/B) in the presence of 1 mM Ca^{2+}/Mg^{2+} (*open bar*), 1 mM Ca^{2+}/Mg^{2+} + 10 μg/ml PT25-2 (*cross-hatched bar*), and 1 mM Mn^{2+} (*filled bar*) is shown. *C*, FITC-Fbg binding to cells expressing αIIb/αV domain-swapping chimeras (TC1C2, TC1, and T) in the presence of 1 mM Ca^{2+}/Mg^{2+} (*open bar*) and 1 mM Mn^{2+} (*filled bar*) and cells pretreated with DTT in the presence of 1 mM Ca^{2+}/Mg^{2+} (*hatched bar*) is shown. *D* and *E*, FITC-Fbg binding to cells expressing αIIb/αV domain-swapping chimeras (T, C1, C2, D, C1C2D, TC2D, TC1D, and TC1C2) in the presence of 1 mM Mn^{2+} (*filled bar*) and cells pretreated with DTT in the presence of 1 mM Ca^{2+}/Mg^{2+} (*hatched bar*) is shown.

αV-propeller joined with αIIb stalk. In terms of cation-binding site, only the site at the junction between the thigh and the calf-1 domains is replaced in those chimeras, and the other four sites in the β-propeller domain remain unchanged (Fig. 1*A*). The chimeras were transiently expressed in CHO cells. Surface expression of each chimeric molecule was monitored using mAbs PL98DF6, P2, SZ21, PT25-2, OP-G2, and AMF-7. All chimeras showed mAb binding comparable with that of wild-type αIIbβ3 or αVβ3 (data not shown). In the presence of 1 mM Ca^{2+}/Mg^{2+} without any activators, none of the cells expressing chimeras including wild-type αIIbβ3 or αVβ3 significantly bound Fbg (Fig. 1*B*). In the presence of mAb PT25-2, which binds to αIIb β-propeller and activates αIIbβ3 (21–23), Fbg bound to wild-type αIIbβ3 and to B/V chimera, but not to wild-type αVβ3 or to V/B chimera. This is because this particular antibody is unable to bind to αVβ3 or V/B. In the presence of 1 mM Mn^{2+}, although αIIbβ3 did show some binding, it was not as avid as that seen in the presence of PT25-2. By contrast, Mn^{2+} induced robust Fbg binding to wild-type αVβ3. These results are in agreement with previous reports. However, when α stalk was swapped, the response to Mn^{2+} changed completely from the wild-type. The B/V bound Fbg just as avidly as wild-type αVβ3. By contrast, V/B binding significantly decreased to a level similar to that of wild-type αIIbβ3. These results clearly indicate that the integrin α stalk, but not the head, contains the critical component that regulates Mn^{2+}-induced integrin activation.

The αV Calf-2 Domain, Not the αIIb Calf-2 Domain, Facilitates Mn^{2+}-induced Activation—To locate the regulatory domain essential for Mn^{2+}-induced activation, we created nine additional domain-swapping chimeras (Fig. 1*A*). These chimeras were created based on the domain boundaries in the αVβ3 crystal structure (3). All of them have αIIb β-propeller on the N terminus. Thus, the ligand-binding domains remain unchanged. Each chimera was designated after the domain replaced, except for the D chimera, which has αV TM and cytoplasmic domains. The chimeras were transiently expressed in CHO cells. Surface expression of each chimera was comparable (data not shown). The first set of experiments showed that TC1C2 bound Fbg just as avidly as B/V in the presence of Mn^{2+} (Fig. 1*C*). However, Mn^{2+} did not induce Fbg binding in TC1 or T. When the cells were pretreated with DTT, which is known to activate integrin, all chimeras including TC1 and T showed Fbg binding comparable to that of wild-type αIIbβ3 in the presence of 1 mM Ca^{2+}/Mg^{2+}. These results suggest that the αV calf-2 domain, but not the αV TM or cytoplasmic domains, is required for Mn^{2+}-induced activation. It is worth noting that none of the chimeras induced constitutive activation. To determine whether αV calf-2 domain alone could facilitate αIIbβ3-Fbg interaction by Mn^{2+}, we swapped individual domains in the next set of experiments. Although swapping individual thigh (T), calf-1 (C1), and TM-cytoplasmic (D) domains had no effect, swapping calf-2 domain (C2) resulted in robust Fbg binding in the presence of Mn^{2+} (Fig. 1*D*). These results suggest that the αV calf-2 domain has a facilitating effect on ligand binding by Mn^{2+}, whereas the αIIb calf-2 domain lacks the same effect. To examine whether αIIb calf-2 domain alone could neutralize the activating effect of α stalk swapping, individual αIIb domain sequences were put back in the B/V chimera that shows Mn^{2+}-induced activation. When original αIIb thigh (C1C2D), calf-1 (TC2D), TM-cytoplasmic (TC1C2) domain sequences were put back in, they did not have a significant effect on Mn^{2+}-induced activation induced by α stalk swapping. However, when αIIb calf-2 domain sequences were put back in (TC1D), the Mn^{2+}-induced activation was completely lost (Fig. 1*E*). This suppressing effect was reversed by DTT treatment. These results suggest that the differences in the response to Mn^{2+} between αIIbβ3 and αVβ3 can be solely attributed to the calf-2 domain.

Mutation in the Cation-binding Site at α Genu Does Not Affect Mn^{2+}-induced Ligand Binding—In the αVβ3 crystal structure, the only cation-binding site in the α stalk is located at the junction between the thigh and the calf-1 domains, but not in the calf-2 domain. To examine the effect of this cation-binding site on ligand binding, Asp^{599} and Glu^{636}, which coor-

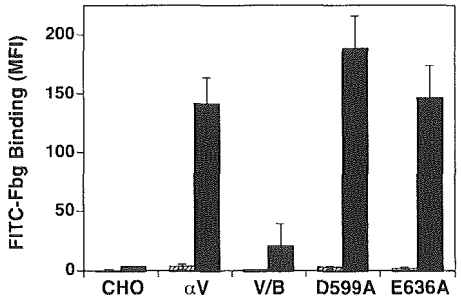

FIG. 2. **The effect of mutation in the cation-coordinating amino acid residues on the αVβ3-ligand interaction.** Asp^{599} and Glu^{636}, which coordinate a cation at αV genu, were individually mutated to Ala. FITC-Fbg binding to CHO cells expressing mutant αVβ3 in the presence of 1 mM Ca^{2+}/Mg^{2+} (*hatched bar*) and 1 mM Mn^{2+} (*filled bar*) is shown.

dinate a cation at αV genu, were mutated to Ala. These two acidic residues are conserved in most integrins. Mutating individual amino acid residues to Ala did not inhibit αVβ3-Fbg interaction induced by Mn^{2+} (Fig. 2). It did not induce constitutive activation in the presence of 1 mM Ca^{2+}/Mg^{2+}, either. Although these results do not rule out the possibility that this cation-binding site may play some role in ligand binding, they are consistent with the results obtained using domain-swapping chimeras.

Specific Amino Acid Residues at the Calf-2/EGF4-βTD Interface Regulate Mn^{2+}-induced Ligand Binding—In the αVβ3 crystal structure, the calf-2 domain creates a 700 Å interface with EGF4 and βTD (24). This implicates that the difference in the interaction between those membrane-proximal domains might affect Mn^{2+}-dependent integrin activation. To explore this possibility, we mutated amino acid residues in the αIIb calf-2 domain that make up the interface. Eight non-conserved amino acid regions (amino acids 747–749, 754–758, 770, 777–779, 783, 893–894, 896–898, and 954–956) that are located at the calf-2/EGF4-βTD interface in the αVβ3 crystal structure were selected. Amino acid sequences in the homologous αIIb regions (amino acids 753–755, 760–764, 774, 781–783, 787, 899–900, 902–904, and 958–960) were replaced with the corresponding αV sequences (designated B/V 753–755, B/V 760–764, B/V 774, B/V 781–783, B/V 787, B/V 899–900, B/V 902–904, and B/V 958–960, respectively). When expressed in CHO cells, all those mutants showed comparable surface expression with wild-type αIIbβ3, except for B/V 902–904, which showed significantly lower expression (data not shown). The DTT treatment induced comparable Fbg binding in all mutants except B/V 902–904. These results suggest that whereas B/V 902–904 has an unfavorable effect on the global structure of αIIbβ3, other mutations did not. In the presence of 1 mM Mn^{2+}, B/V 753–755, B/V 774, B/V 781–783, B/V 902–904, or B/V 958–960 showed comparable Fbg binding with wild-type αIIbβ3 (Fig. 3*A*). In contrast, B/V 787 and B/V 899–900 showed significantly higher Fbg binding. In addition, B/V 760–764 also showed weak but consistently higher Fbg binding than wild-type αIIbβ3. To further identify the amino acid residues in the 760–764 and 899–900 regions important for Mn^{2+}-induced Fbg binding, individual residues in these regions were mutated. None of the single amino acid mutations in the 760–764 region induced Fbg binding equivalent to B/V 760–764. On the contrary, mutating Arg^{900} to Ser alone was sufficient to induce Fbg binding equivalent to B/V 899–900 (Fig. 3*B*). However, none of those mutations produced Fbg binding as robust as C2. Next we examined whether combining those mutations would have an additive or synergistic effect. Combining B/V 787 mutation with the B/V 899–900 or B/V 900 mutation (designated B/V 787/899–900 and B/V 787/900, respectively) did not have any significant effect (Fig. 3*C*). The effect of combining B/V 760–764 mutation with B/V 787/899–900 (designated B/V 760–764/787/899–900) was additive and resulted in higher Fbg binding than any one of these mutants. These results indicate that whereas B/V 787 and B/V 900 have similar effects, B/V 760–764 has an independent effect on Mn^{2+}-induced Fbg binding. In the αVβ3 crystal structure, amino acid residues 783 and 894, which correspond to 787 and 900 in αIIb, are located next to each other and make contacts with the EGF4 domain, whereas 754–758, which corresponds to 760–764 in αIIb, is located close to the cell membrane and makes contacts with the βTD (Fig. 3*D*). These results indicate that the effect of calf-2 domain swapping on the Mn^{2+}-induced ligand interaction is mediated at least in part by the specific amino acid residues in the calf-2/EGF4-βTD interface, suggesting that differences in the calf-2/EGF4 and calf-2/βTD interface interaction in two β3 integrins are indeed responsible for the distinct response to Mn^{2+}. However, the fact that combining B/V 760–764, B/V 787, and B/V 899–900 mutations did not produce as much Fbg binding as C2 indicates that other amino acid residues in the calf-2 domain are involved. The positions of amino acid residues 839–867 in the αV calf-2 domain (842–873 in αIIb) have not been assigned in the αVβ3 crystal structure. This region may provide additional sites important for regulating integrin-ligand interaction.

Constraining the Calf-2/EGF4-βTD Interface in αVβ3 Inhibits Mn^{2+}-induced Activation—If calf-2/EGF4-βTD interface interaction is involved in the regulation of Mn^{2+}-induced ligand binding, constraint in the interface should have a profound impact on integrin activation and conformation. To examine this hypothesis, we introduced an artificial disulfide bridge to put constraint in this interface. As seen in Fig. 4*A*, αV Ser^{749} and β3 Asp^{606} are physically close, and if these residues are mutated to Cys at the same time, we will be able to introduce a disulfide bridge. Although individual αV S749C or β3 D606C did not have any significant effect, double cysteine mutation 749/606 reduced Fbg binding to about one-third (Fig. 4*B*). This suppression was neutralized when the cells were treated with DTT to disrupt the disulfide bridge. These results suggest that restraining the possible movements in this membrane-proximal domain interface has a significant inhibitory effect on Mn^{2+}-induced integrin activation.

Next we examined the effect of the constraint on the conformational change of αVβ3. To monitor the conformational change, we examined the binding of anti-LIBS antibodies. The anti-LIBS mAbs bind preferentially to ligand-occupied form of integrins. Thus, they are believed to detect conformational changes associated with ligand binding (19). In this assay, the binding of non-functional anti-β3 mAb VNR5-2 did not change among those mutants. The presence of 1 mM GRGDS peptide did not significantly affect the binding, either (Fig. 4*C*). The binding of anti-LIBS1 was significantly weaker than that of VNR5-2. However, the binding of anti-LIBS1 showed a robust increase in the presence of 1 mM GRGDS peptide. No significant difference was observed among wild-type and cysteine mutants (Fig. 4*D*). By contrast, anti-LIBS2 binding in the presence of GRGDS peptide was suppressed in the double mutant (Fig. 4*E*). Although the localization of the epitope for anti-LIBS1 is not known, the epitope for anti-LIBS2 has been located within amino acid residues 602–690 in the βTD (25). These results suggest that the constraint on the membrane-proximal α/β interface restricts the conformational change within the membrane-proximal domain upon ligand binding. However, it may not prevent the conformational change in other parts of the molecule.

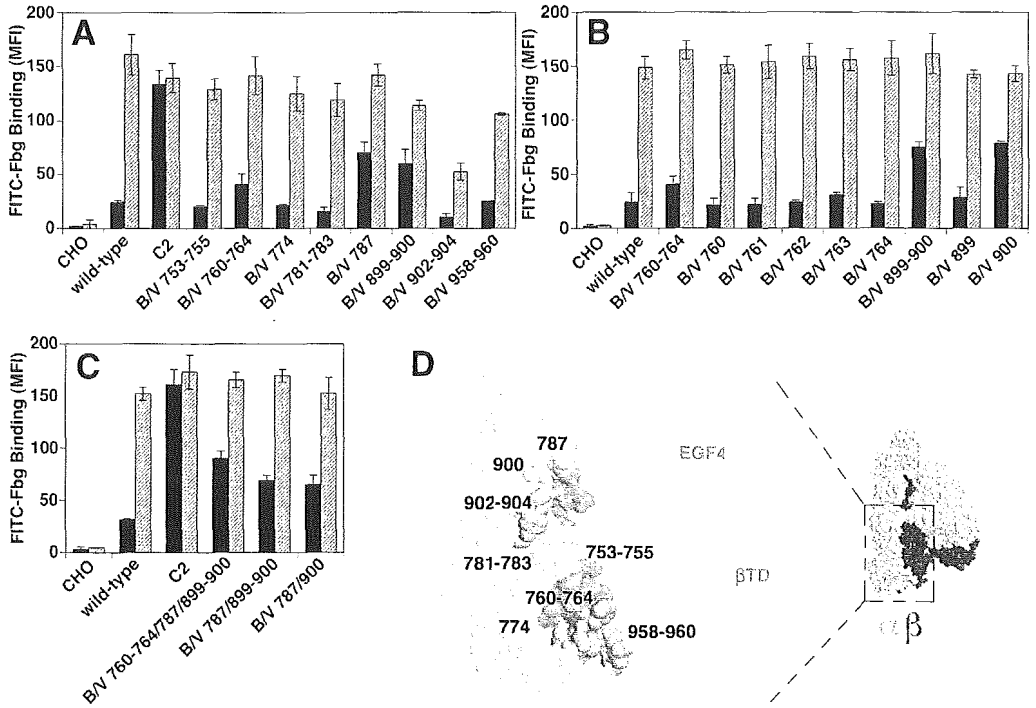

FIG. 3. **The effect of αIIb to αV mutation in amino acid residues located at the calf-2/EGF4-βTD interface on the αIIbβ3-ligand interaction.** *A*, amino acid residues 753–755, 760–764, 774, 781–783, 787, 899–900, 902–904, and 958–960 located at the calf-2/EGF4-βTD interface in αIIb were mutated to the corresponding residues in αV. The resulting αIIbβ3 mutants are designated B/V 753–755, B/V 760–764, B/V 774, B/V 781–783, B/V 787, B/V 899–900, B/V 902–904, and B/V 958–960, respectively. *B*, amino acid residues in the αIIb 760–764 and 899–900 regions were individually mutated to the corresponding residues in αV. *C*, B/V 760–764, B/V 787, and B/V 899–900 or B/V 900 mutations were combined. These αIIbβ3 mutants were expressed in CHO cells. FITC-Fbg binding to cells expressing αIIbβ3 in the presence of 1 mM Mn^{2+} (*filled bar*) and cells pretreated with DTT in the presence of 1 mM Ca^{2+}/Mg^{2+} (*hatched bar*) is shown. As a reference, Fbg binding to cells expressing wild-type αIIbβ3 and C2 chimera are also shown. *D*, the spacefill model of αVβ3 crystal structure. The αV chain is shown in *green*, and the β3 chain is shown in *red*. The membrane-proximal domains are magnified on the *left*. The calf-2 domain is shown in *light green*, and the EGF4 and βTD are shown in *transparent red*. Positions of amino acid residues corresponding to 753–755, 760–764, 774, 781–783, 787, 900, 902–904, and 958–960 in αIIb are shown and labeled. Amino acid residues 787/900 and 760–764, which promoted Mn^{2+}-induced Fbg binding when mutated to αV residue, are shown in *yellow* and *orange*, respectively. Amino acid residues 753–755, 774, and 781–783, which did not affect Fbg binding, are in *cyan*. Amino acid residues 902–904, which jeopardized surface expression and Fbg binding, are shown in *blue*. The models were created using RasMol.

Constraint in the Calf-2/EGF4-βTD Interface in αIIbβ3 Completely Abrogates Inside-out Signaling—We next examined the effect of this interdomain interaction on integrin activation induced by other stimuli. We introduced homologous cysteine mutation into αIIbβ3 and examined the effect on Fbg binding in the presence of 1 mM Ca^{2+}/Mg^{2+} (Fig. 5*A*). Without activators, none of those mutants bound Fbg. When activating mAb PT25-2 was included to enforce the conformational change of the extracellular domain in favor of ligand binding, wild-type (αIIb/β3) and individual cysteine mutants αIIb F755C (755/β3) and β3 D606C (αIIb/606) showed comparable Fbg binding. However, the Fbg binding to double cysteine mutant 755/606 showed a 50% decrease. The effect of the constraint was neutralized when the disulfide bridge was disrupted by prior treatment with DTT. These results suggest that constraining the membrane-proximal domain interface prevents integrin from achieving full activation, regardless of activators.

The effect of the constraint is far more dramatic in inside-out signaling. To mimic inside-out signaling, the cytoplasmic domain of β3 was truncated at the membrane-proximal Leu^{717} (26). The truncated αIIbβ3 (αIIb/β3tr) bound Fbg in the presence of Ca^{2+}/Mg^{2+} without any activators, as reported previously (Fig. 5*B*). When individual cysteine mutation αIIb F755C or β3 D606C was introduced in truncated αIIbβ3 (designated 755/β3tr and αIIb/606tr, respectively), it did not significantly block Fbg binding. In contrast, Fbg binding was completely abrogated in double cysteine mutant 755/606tr. Activating antibody did not override the inhibition completely. Fbg binding was completely restored only when the disulfide bridge was disrupted with DTT treatment. The cysteine mutations had similar effects when αIIbβ3 was activated by αIIb cytoplasmic domain truncation (Fig. 5*C*). Although individual αIIb F755C or β3 D606C mutation (775tr/β3 and αIIbtr/606, respectively) did not have a significant impact as compared with wild-type (αIIbtr/β3), double cysteine mutation 755tr/606 completely abrogated Fbg binding. This suppression was completely neutralized with DTT treatment. Thus, disruption of the membrane-proximal domain interface is essential for propagating inside-out signaling. These results suggest that constraining the membrane-proximal α/β interface not only restricts integrin activation by divalent cations but also prevents activation by inside-out signaling.

DISCUSSION

In this study, we provide evidence that interdomain interactions in the integrin stalk regions, particularly in the membrane-proximal domains, are the key regulator of integrin activation. By using Mn^{2+}-induced Fbg binding to β3 integrins as a model system, we demonstrated the following: 1) that switching α stalk region resulted in switching the Mn^{2+} requirement for ligand binding in αIIbβ3 and αVβ3, 2) that the calf-2 domain in the α stalk region is the sole determinant for the distinct response to Mn^{2+}, 3) that this response is mediated in part by the specific amino acid residues in the calf-2 domain that create the calf-2/EGF4-βTD interface, and 4) that constraining the calf-2/EGF4-βTD interface not only inhibited Mn^{2+}-induced integrin activation but also completely abrogated inside-out signaling. These results suggest that the ex-

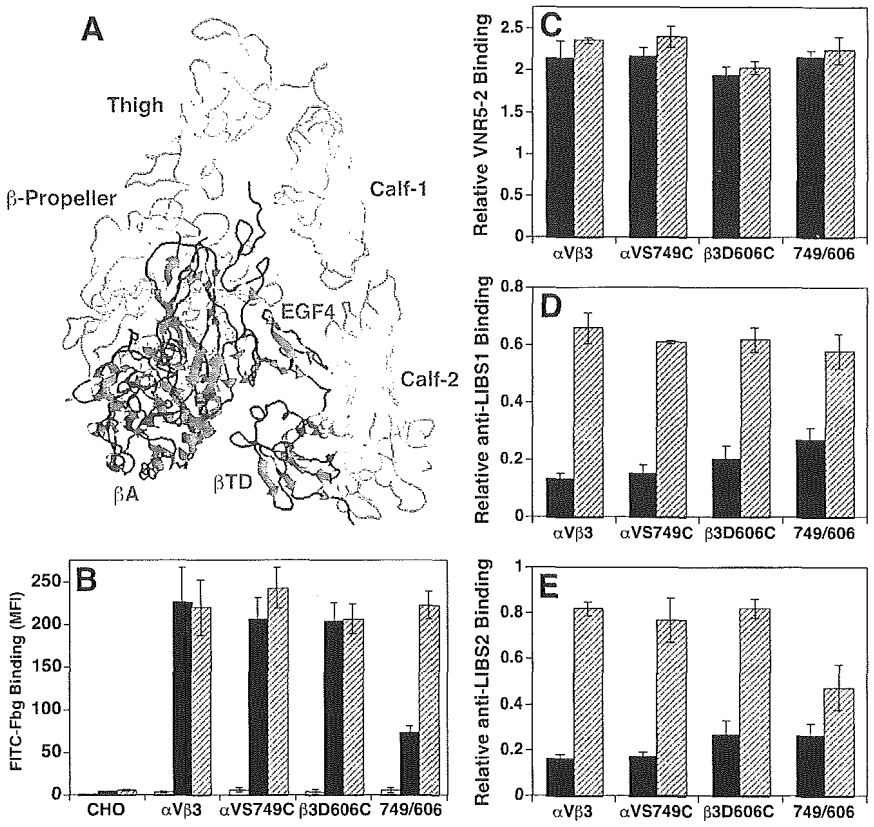

FIG. 4. **The effect of constraint in the membrane-proximal α/β interface in $\alpha V\beta 3$ on ligand binding and conformation.** *A*, ribbon models depicting the crystal structure of the $\alpha V\beta 3$ extracellular domain. The α and β subunits are shown in *cyan* and *red*, respectively. The amino acid residues Ser^{749} in αV and Asp^{606} in $\beta 3$ that were mutated to Cys to facilitate disulfide bridge formation in the study are shown in *yellow* and *orange spacefills*, respectively. The model was created using RasMol. *B*, FITC-Fbg binding to cells expressing individual Cys mutant αVS749C, β3D606C, and double Cys mutant 749/606 in the presence of 1 mM Ca^{2+}/Mg^{2+} (*open bar*) and 1 mM Mn^{2+} (*filled bar*) and cells pretreated with DTT in the presence of 1 mM Mn^{2+} (*hatched bar*) is shown. *C–E*, mAb binding to cells expressing individual Cys mutant αVS749C, β3D606C, and double Cys mutant 749/606 in the presence 1 mM Ca^{2+}/Mg^{2+} (*filled bar*) and 1 mM Ca^{2+}/Mg^{2+} + 1 mM GRGDS peptide (*hatched bar*) is shown. Relative mAb binding was calculated as described under "Experimental Procedures." The binding of VNR5-2, anti-LIBS1, anti-LIBS2 is shown in *C*, *D*, and *E*, respectively.

tracellular, membrane-proximal α/β interaction plays important roles in regulating the cation-dependent integrin activation and critically controls the propagation of inside-out signaling.

Integrin α subunit contains five cation-binding sites. The four EF-hand-like motifs in α subunit previously predicted to bind Ca^{2+} form β hairpin loops and actually coordinate cations regardless of bound ligand (3). Although previous studies have shown that the Fbg γ-chain peptide cross-links to the second EF-hand-like motif in blade 5 of the αIIb-propeller (27), mutational studies suggest these sites are not likely to contain a major ligand-binding site (28, 29). In addition, conservative Asp/Asn to Glu mutations in the four EF-hand-like motifs in $\alpha 4\beta 1$ had no effect on the binding of soluble ligand (30). Consistently, these β hairpin loops are all located opposite to the β-propeller/βA interface that comprises the ligand binding face. Our results using α stalk-swapping mutants suggest that the β-propeller domain does not contain a regulatory site for Mn^{2+}-induced Fbg binding, but the α stalk does. Indeed, the α stalk contains the fifth cation-binding site at the junction between the thigh and calf-1 domains. This site is located at the α genu, where integrin makes a 135° bend in the crystal structure. It has been predicted that a cation bound to this site may help neutralize the negative charge in the thigh/calf-1 interface in an extended conformer (3). Thus, it is tempting to speculate that this cation-binding site may regulate Mn^{2+}-induced ligand binding by controlling the transition from bent to extended conformer. However, our results suggest this is not the case. Instead, results from the domain-swapping chimeras indicate that the C-terminal α calf-2 domain plays a critical role in regulating integrin activation.

Several lines of evidence implicate the role of the calf-2 domain in integrin activation. Some integrin α subunit is proteolytically cleaved into covalently linked heavy and light chains during post-translational processing. Prevention of this endoproteolytic cleavage by mutagenesis abrogated $\alpha 6\beta 1$ activation by phorbol myristate acetate (31). Neutrophil elastase cleaves αIIb between Val^{837} and Asp^{838}, close to the endoproteolytic cleavage site in the calf-2 domain (32). Although the elastase does not, by itself, induce platelet aggregation, it greatly potentiates $\alpha IIb\beta 3$ activation by cathepsin G and Mn^{2+} (17, 33). Thus, structural alterations in the calf-2 domain affect integrin activation. Conversely, ligand binding provokes structural change in the calf-2 domain. Upon ligand binding, the integrin stalk regions express neo-epitopes that are recognized by a group of anti-LIBS mAbs. These epitopes are mostly located in the β stalk region (25, 34). Notably, one such mAb, PMI-1, recognizes an epitope within residues 842–856 of the αIIb calf-2 domain (35). Thus, structural change in the calf-2 domain is closely associated with integrin activation. How does the calf-2 domain affect Mn^{2+}-induced Fbg binding, despite the fact that it does not contain actual cation-binding sites? Previous studies suggest that the membrane-proximal α/β interaction modulates integrin affinity regulation by divalent cations. Kinetic studies using recombinant truncated $\alpha 5\beta 1$ and $\alpha V\beta 3$ with an artificial C-terminal clasp suggest that α/β interaction in the TM and cytoplasmic domains decreases integrin affinity by increasing the dissociation rate. Electron microscopic observation revealed that the two stalks are widely separated at their ends in unclasped $\alpha 5\beta 1$ (36), whereas they are still connected at their ends in a majority of molecules in unclasped recombinant $\alpha V\beta 3$, even in the presence of Mn^{2+} (4). These reports suggest that the extracellular, membrane-proximal α/β interface formation is significant in some integrins under physiological conditions and may account for the distinct response to Mn^{2+} in $\beta 3$ integrins. Indeed, αIIb to αV mutation in selected amino acid residues that make up the calf-2/EGF4 and calf-2/βTD interface greatly facilitated Mn^{2+}-induced Fbg binding in $\alpha IIb\beta 3$. Stabilizing this interface with a disulfide bridge (749/606 mutant) prevented Mn^{2+}-induced Fbg binding to $\alpha V\beta 3$. It is possible that constraining the membrane-proximal α/β interface may somehow constrain integrin in a bent

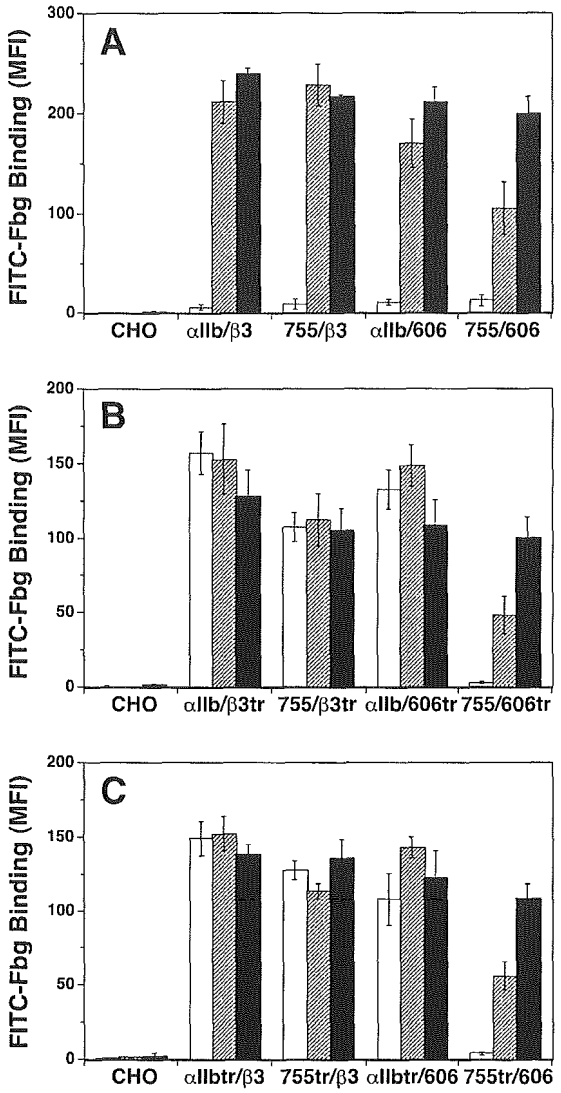

FIG. 5. **The effect of constraint in the membrane-proximal α/β interface on ligand binding to $\alpha IIb\beta 3$.** *A*, amino acid residue Phe^{755} in αIIb, which is homologous to Ser^{749} in αV, was mutated to Cys (F755C) to facilitate disulfide bridge formation between αIIb and β3. FITC-Fbg binding to cells expressing αIIbβ3 (*αIIb/β3*) carrying individual αIIb F755C mutation (*755/β3*), β3 D606C mutation (*αIIb/606*), and double αIIb F755C and β3 D606C mutation (*755/606*) in the presence of 1 mM Ca^{2+}/Mg^{2+} (*open bar*) and 1 mM Ca^{2+}/Mg^{2+} plus 10 μg/ml PT25-2 (*hatched bar*) and cells pretreated with DTT in the presence of 1 mM Ca^{2+}/Mg^{2+} (*filled bar*) is shown. *B*, to mimic inside-out signaling, β3 was truncated at Leu^{717} by introducing a stop codon in β3 cDNA (β3tr). The D606C mutation was introduced in β3tr (606tr). Wild-type αIIb or αIIb carrying F755C mutation was expressed together with β3tr or 606tr in CHO cells. FITC-Fbg binding to cells expressing truncated αIIbβ3 (*αIIb/β3tr*) carrying αIIb F755C mutation (*755/β3tr*), β3 D606C mutation (*αIIb/606tr*), and αIIb F755C and β3 D606C mutations (*755/606tr*) in the presence of 1 mM Ca^{2+}/Mg^{2+} (*open bar*) and 1 mM Ca^{2+}/Mg^{2+} plus 10 μg/ml PT25-2 (*hatched bar*) and cells pretreated with DTT in the presence of 1 mM Ca^{2+}/Mg^{2+} (*filled bar*) is shown. *C*, to mimic inside-out signaling, αIIb was truncated at Gly^{991} by introducing a stop codon in αIIb cDNA (αIIbtr). The F755C mutation was introduced in αIIbtr (755tr). Wild-type β3 or β3 carrying the D606C mutation was expressed together with αIIbtr or 755tr in CHO cells. FITC-Fbg binding to cells expressing truncated αIIbβ3 (*αIIbtr/β3*) carrying αIIb F755C mutation (*755tr/β3*), β3 D606C mutation (*αIIbtr/606*), and αIIb F755C and β3 D606C mutations (*755tr/606*) in the presence of 1 mM Ca^{2+}/Mg^{2+} (*open bar*) and 1 mM Ca^{2+}/Mg^{2+} plus 10 μg/ml PT25-2 (*hatched bar*) and cells pretreated with DTT in the presence of 1 mM Ca^{2+}/Mg^{2+} (*filled bar*) is shown.

state, thereby keeping integrin in a low affinity state. However, the 749/606 and 755/606 double mutants did undergo conformational change upon ligand binding, as detected by LIBS epitope expression. These mutants still showed some Fbg binding when stimulated by Mn^{2+} or activating mAb. In contrast, constraining the integrin in a bent state by introducing a disulfide bridge between βA and βTD resulted in failure to induce LIBS epitope expression upon ligand binding and complete loss of ligand binding, even in the presence of activating mAb.[2] Thus, constraining the α/β stalks and β head/β stalk has a distinct conformational effect on integrin structure. In addition, the fact that extended, clasped conformer can be observed under electron microscopy (4) indicates that constraining the α/β stalks does not necessarily constrain integrin in a bent state. On the contrary, disruption of the membrane-proximal α/β interface may lead to integrin activation. Anti-LIBS2 that binds to βTD has been shown to activate αIIbβ3 (25). Likewise, two mAbs that bind to αIIb calf-2 domain weakly induced Fbg binding in the presence of Ca^{2+}/Mg^{2+}. Notably, these mAbs potentiated Mn^{2+}-induced Fbg binding.[3] Disruption of the Cys^{608}-Cys^{655} and Cys^{663}-Cys^{687} disulfide bridges in βTD that face the calf-2/EGF4-βTD interface in the crystal structure constitutively activated αIIbβ3, whereas disruption of the other two disulfide bridges did not (37). These results implicate that the membrane-proximal calf-2/EGF4-βTD interface may act as a physiological clasp and thus regulate integrin activation.

Integrin stalks also make interface at calf-1/EGF3, TM domains, and cytoplasmic tails. Previous studies suggest that α/β interaction in TM domain and cytoplasmic tail, as well as the interaction of cytoplasmic tails with actin cytoskeleton, is important for restraining integrins in low affinity form (38–41). These membrane-proximal interactions probably act in concert to maintain integrin in the default low affinity state because disruption of any of these interactions makes the integrin prone to activation. This may explain why the detergent-solubilized or truncated recombinant αIIbβ3 is able to bind ligands without activation, whereas intact heterodimers on the platelet surface are not able to do so. Among α/β interfaces, calf-2/EGF4-βTD is unique because only the calf-2 domain (and not the thigh, calf-1, or TM-cytoplasmic domains) displayed a significant difference in promoting Mn^{2+}-induced integrin activation, suggesting that this interface is much more stable in αIIbβ3 than in αVβ3. The divergent nature of the calf-2/EGF4-βTD interface interaction among integrins may be responsible for the different LIBS epitope expression in β1 integrins in response to ligand or Mn^{2+} occupancy (42). Thus, the calf-2/EGF4-βTD interaction may differentially regulate ligand interaction and conformational change in integrins.

In inside-out signaling, how the interactions within the short cytoplasmic tails trigger structural rearrangements in the large extracellular domain remains a mystery. The cytoplasmic, membrane-proximal interaction constrains integrin in an inactive state (40). Recently, the talin head domain has been shown to activate αIIbβ3 by disrupting the membrane-proximal αIIb/β3 tail interface *in vitro* (43). In living cells, the αL/β2 cytoplasmic tails undergo separation upon agonist stimulation (44). Conversely, in outside-in signaling, ligand binding induces a structural rearrangement in the cytoplasmic tails and induces separation of the tails (44) and exposure of the LIBS epitope in α tail (45). Our results unequivocally indicate that separation of the cytoplasmic tails is unable to induce integrin activation unless the extracellular stalks separate from each other. In agreement, previous studies have shown that αIIbβ3 stalks undergo structural rearrangement and

[2] T. Kamata, M. Handa, Y. Ikeda, and S. Aiso, manuscript in preparation.

[3] T. Kamata, M. Handa, Y. Ikeda, and S. Aiso, unpublished observations.

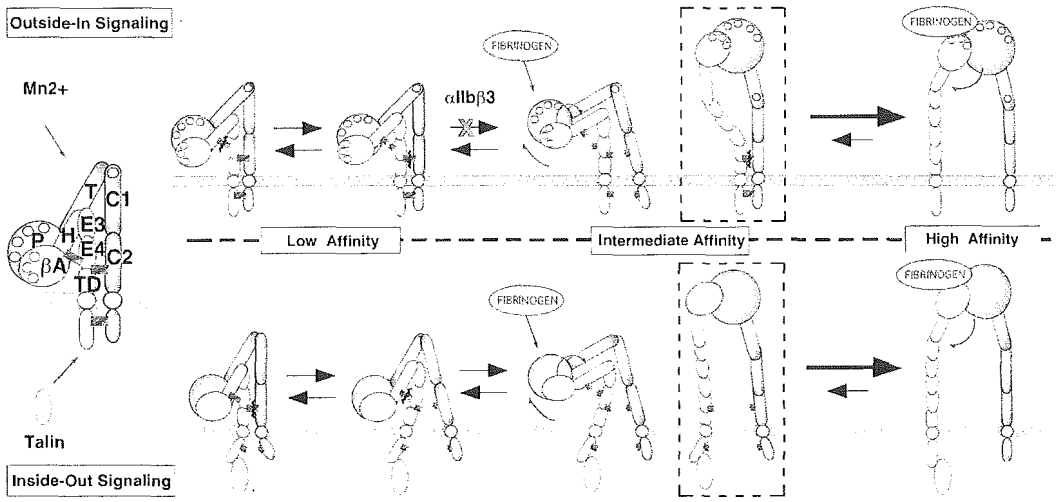

FIG. 6. **A relay switch model of integrin activation.** The α and β subunits are illustrated in *blue* and *green*, respectively. The β-propeller, *thigh*, *calf-1*, and *calf-2* domains in α are labeled as *P*, *T*, *C1*, and *C2*, respectively, and the βA, hybrid, EGF3, EGF4, and βTD domains in β are labeled as *βA*, *H*, *E3*, *E4*, and *TD*, respectively. The PSI, EGF1, and EGF2 domains in β are not shown for simplicity. The putative interactions in the β head/β stalk, α stalk/β stalk, and α cytoplasmic tail/β cytoplasmic tail interfaces are shown as a *red bar*. The eight cation-binding sites are shown as *white circles*. Manganese ions are depicted as *yellow circles*. Destabilization and disruption of the interface are shown as a *black* and a *white break* in the bar, respectively. The low affinity form is depicted as bent conformer. The high affinity form is depicted as extended, open, unclasped conformer. The hypothetical intermediate affinity forms in β3 integrin are depicted as the bent, unclasped form. Alternatively, the extended, closed, clasped form (in outside-in signaling) and the extended, closed, unclasped form (in inside-out signaling) shown within the *broken rectangle* may be the predominant intermediates in other integrins. All conformers are in structural equilibrium with each other. The presence of ligands shifts the equilibrium toward the formation of the high affinity conformer.

change their relative distance or orientation on the cell surface upon agonist stimulation of platelets (46). Thus, disruption of the calf-2/EGF4-βTD interface that follows the α/β cytoplasmic tail separation triggers a cascade of structural rearrangement of integrin extracellular domains in inside-out signaling. Most likely, disruption of the calf-2/EGF4-βTD interface would be required for the propagation of outside-in signaling as well.

Based on the results from the current and previous studies, we propose a relay switch model of integrin activation (Fig. 6). The β stalk makes extensive interfaces not only with α stalk but also with β head composed of βA and β hybrid domains. These multiple interactions involving the β stalk seem to constrain integrin in the inactive form because disruption of virtually any disulfide bridge in the four EGF domains constitutively activates αIIbβ3 (47). In this model, the α/β stalk and the β head/stalk interactions are physically linked, functioning as a relay switch to transmit conformational signals from one end to the other: disruption of the α/β stalk interface destabilizes the β head/stalk interface and vice versa. In inside-out signaling (Fig. 6, *bottom panel*), interaction of integrin cytoplasmic tails with intracellular proteins such as talin disrupts the α/β cytoplasmic tail and the TM domain interfaces. This triggers the disruption of the α/β stalk interface that would destabilize the β head/stalk interface. Destabilization of the β head/stalk interface releases the βA-hybrid domains from the constraint that prevents the swing-out of the hybrid domain, thus greatly potentiating integrin activation. However, this may not be sufficient to induce extension because mAb cross-competition studies implicate that αIIbβ3 still assumes a bent conformer on agonist-stimulated platelets (48). Consistently, agonist stimulation alone is not sufficient but requires ligand binding to induce LIBS epitope expression in platelet αIIbβ3 (19, 49). Thus, ligand binding and the associated swing-out of the hybrid domain may give an additional push to the structural transition. Alternatively, α/β stalk separation may be able to induce significant integrin extension without swing-out of the hybrid domain (extended, closed headpiece), facilitating the access of macromolecular ligands. In outside-in signaling (Fig. 6, *top panel*), Mn^{2+} binding to the βA domain may be able to induce a conformational change in the β head sufficient to destabilize the β head/stalk interface. This triggers destabilization of the α/β stalk interface, which further makes the β head/stalk interface unstable, potentiating integrin activation. With increased affinity, the binding of ligands facilitates swing-out of the β hybrid domain (50), which would completely disrupt the β head/stalk interface and allow the integrin to extend, followed by complete separation of the α/β stalk, exposing the binding sites for signaling molecules in the cytoplasmic tails. However, tight interaction in the calf-2/EGF4-βTD interface prevents destabilization in the β head/stalk interface and keeps integrin in the low affinity state in αIIbβ3. Alternatively, Mn^{2+} alone may be able to induce integrin extension without releasing the C-terminal clasp (extended, closed headpiece). Ligand binding following Mn^{2+} occupancy induces swing-out of the β hybrid domain that promotes the release of the C-terminal clasp (extended, open headpiece). The extended, closed form may be predominant in β1 and β2 integrins because Mn^{2+} alone induces significant LIBS epitope expression (42). By contrast, Mn^{2+} does not induce significant LIBS epitope expression in β3 integrins (data not shown). This model explains how structural signals initiated in the C-terminal tail and the N-terminal ligand-binding head propagate to each other.

Our results suggest that any endogenous molecules or reagents that potentially affect α/β interface formation may modulate integrin activation. Indeed, CD151, platelet-derived growth factor receptor β, vascular endothelial growth factor receptor 2, and CD47 have been shown to associate with integrin extracellular domains (51–54). These molecules may affect integrin activation by interfering with or stabilizing intersubunit or intrasubunit interface formation by binding to integrin stalks. Likewise, chemicals or reagents that cross-link and stabilize the calf-2/EGF4-βTD interface will be able to selectively inhibit inside-out signaling (and probably outside-in signaling as well) without inhibiting low affinity ligand binding or inducing LIBS epitope expression. Thus, membrane-proximal α/β interaction can be a novel target for effective anti-integrin therapies.

Acknowledgments—We thank Dr. Joseph C. Loftus for providing αIIb, αV, and β3 cDNAs; Drs. Mark H. Ginsberg, Jari Ylänne, Ismo Virtanen, and Yoshiaki Tomiyama for providing anti-αIIbβ3 mAbs; and Sonomi Ito for excellent technical assistance.

REFERENCES

1. Hynes, R. O. (2002) *Cell* **110,** 673–687
2. Weisel, J. W., Nagaswami, C., Vilaire, G., and Bennett, J. S. (1992) *J. Biol. Chem.* **267,** 16637–16643
3. Xiong, J. P., Stehle, T., Diefenbach, B., Zhang, R., Dunker, R., Scott, D. L., Joachimiak, A., Goodman, S. L., and Arnaout, M. A. (2001) *Science* **294,** 339–345
4. Takagi, J., Petre, B. M., Walz, T., and Springer, T. A. (2002) *Cell* **110,** 599–611
5. Luo, B. H., Springer, T. A., and Takagi, J. (2003) *Proc. Natl. Acad. Sci. U. S. A.* **100,** 2403–2408
6. Chigaev, A., Zwartz, G. J., Buranda, T., Edwards, B. S., Prossnitz, E. R., and Sklar, L. A. (2004) *J. Biol. Chem.* **279,** 32435–32443
7. Chigaev, A., Buranda, T., Dwyer, D. C., Prossnitz, E. R., and Sklar, L. A. (2003) *Biophys. J.* **85,** 3951–3962
8. Mould, A. P., Akiyama, S. K., and Humphries, M. J. (1995) *J. Biol. Chem.* **270,** 26270–26277
9. Loftus, J. C., O'Toole, T. E., Plow, E. F., Glass, A., Frelinger, A. L., III, and Ginsberg, M. H. (1990) *Science* **249,** 915–918
10. Kamata, T., Tieu, K. K., Tarui, T., Puzon-McLaughlin, W., Hogg, N., and Takada, Y. (2002) *J. Immunol.* **168,** 2296–2301
11. Xiong, J. P., Stehle, T., Zhang, R., Joachimiak, A., Frech, M., Goodman, S. L., and Arnaout, M. A. (2002) *Science* **296,** 151–155
12. Chen, J., Salas, A., and Springer, T. A. (2003) *Nat. Struct. Biol.* **10,** 995–1001
13. Fitzgerald, L. A., Poncz, M., Steiner, B., Rall, S. C., Jr., Bennett, J. S., and Phillips, D. R. (1987) *Biochemistry* **26,** 8158–8165
14. Smith, J. W., Piotrowicz, R. S., and Mathis, D. (1994) *J. Biol. Chem.* **269,** 960–967
15. Yan, B., Hu, D. D., Knowles, S. K., and Smith, J. W. (2000) *J. Biol. Chem.* **275,** 7249–7260
16. Marguerie, G. A., Edgington, T. S., and Plow, E. F. (1980) *J. Biol. Chem.* **255,** 154–161
17. Azuma, H., Shigekiyo, T., Miura, S., Uno, Y., and Saito, S. (1989) *Thromb. Haemostasis* **62,** 984–988
18. Ylanne, J., Hormia, M., Jarvinen, M., Vartio, T., and Virtanen, I. (1988) *Blood* **72,** 1478–1486
19. Frelinger, A. L., III, Cohen, I., Plow, E. F., Smith, M. A., Roberts, J., Lam, S. C., and Ginsberg, M. H. (1990) *J. Biol. Chem.* **265,** 6346–6352
20. Tomiyama, Y., Tsubakio, T., Piotrowicz, R. S., Kurata, Y., Loftus, J. C., and Kunicki, T. J. (1992) *Blood* **79,** 2303–2312
21. Tokuhira, M., Handa, M., Kamata, T., Oda, A., Katayama, M., Tomiyama, Y., Murata, M., Kawai, Y., Watanabe, K., and Ikeda, Y. (1996) *Thromb. Haemostasis* **76,** 1038–1046
22. Kamata, T., Irie, A., Tokuhira, M., and Takada, Y. (1996) *J. Biol. Chem.* **271,** 18610–18615
23. Puzon-McLaughlin, W., Kamata, T., and Takada, Y. (2000) *J. Biol. Chem.* **275,** 7795–7802
24. Xiong, J. P., Stehle, T., Goodman, S. L., and Arnaout, M. A. (2003) *J. Thromb. Haemostasis* **1,** 1642–1654
25. Du, X., Gu, M., Weisel, J. W., Nagaswami, C., Bennett, J. S., Bowditch, R., and Ginsberg, M. H. (1993) *J. Biol. Chem.* **268,** 23087–23092
26. Hughes, P. E., O'Toole, T. E., Ylanne, J., Shattil, S. J., and Ginsberg, M. H. (1995) *J. Biol. Chem.* **270,** 12411–12417
27. D'Souza, S. E., Ginsberg, M. H., Burke, T. A., and Plow, E. F. (1990) *J. Biol. Chem.* **265,** 3440–3446
28. Gidwitz, S., Lyman, S., and White, G. C., II. (2000) *J. Biol. Chem.* **275,** 6680–6688
29. Kamata, T., Tieu, K. K., Irie, A., Springer, T. A., and Takada, Y. (2001) *J. Biol. Chem.* **276,** 44275–44283
30. Pujades, C., Alon, R., Yauch, R. L., Masumoto, A., Burkly, L. C., Chen, C., Springer, T. A., Lobb, R. R., and Hemler, M. E. (1997) *Mol. Biol. Cell* **8,** 2647–2657
31. Delwel, G. O., Hogervorst, F., and Sonnenberg, A. (1996) *J. Biol. Chem.* **271,** 7293–7296
32. Si-Tahar, M., Pidard, D., Balloy, V., Moniatte, M., Kieffer, N., Van Dorsselaer, A., and Chignard, M. (1997) *J. Biol. Chem.* **272,** 11636–11647
33. Renesto, P., and Chignard, M. (1993) *Blood* **82,** 139–144
34. Honda, S., Tomiyama, Y., Pelletier, A. J., Annis, D., Honda, Y., Orchekowski, R., Ruggeri, Z., and Kunicki, T. J. (1995) *J. Biol. Chem.* **270,** 11947–11954
35. Loftus, J. C., Plow, E. F., Frelinger, A. L., III, D'Souza, S. E., Dixon, D., Lacy, J., Sorge, J., and Ginsberg, M. H. (1987) *Proc. Natl. Acad. Sci. U. S. A.* **84,** 7114–7118
36. Takagi, J., Erickson, H. P., and Springer, T. A. (2001) *Nat. Struct. Biol.* **8,** 412–416
37. Butta, N., Arias-Salgado, E. G., Gonzalez-Manchon, C., Ferrer, M., Larrucea, S., Ayuso, M. S., and Parrilla, R. (2003) *Blood* **102,** 2491–2497
38. Li, R., Mitra, N., Gratkowski, H., Vilaire, G., Litvinov, R., Nagasami, C., Weisel, J. W., Lear, J. D., DeGrado, W. F., and Bennett, J. S. (2003) *Science* **300,** 795–798
39. Hughes, P. E., Diaz-Gonzalez, F., Leong, L., Wu, C., McDonald, J. A., Shattil, S. J., and Ginsberg, M. H. (1996) *J. Biol. Chem.* **271,** 6571–6574
40. Lu, C., Takagi, J., and Springer, T. A. (2001) *J. Biol. Chem.* **276,** 14642–14648
41. Bennett, J. S., Zigmond, S., Vilaire, G., Cunningham, M. E., and Bednar, B. (1999) *J. Biol. Chem.* **274,** 25301–25307
42. Bazzoni, G., Ma, L., Blue, M. L., and Hemler, M. E. (1998) *J. Biol. Chem.* **273,** 6670–6678
43. Vinogradova, O., Velyvis, A., Velyviene, A., Hu, B., Haas, T., Plow, E., and Qin, J. (2002) *Cell* **110,** 587–597
44. Kim, M., Carman, C. V., and Springer, T. A. (2003) *Science* **301,** 1720–1725
45. Leisner, T. M., Wencel-Drake, J. D., Wang, W., and Lam, S. C. (1999) *J. Biol. Chem.* **274,** 12945–12949
46. Sims, P. J., Ginsberg, M. H., Plow, E. F., and Shattil, S. J. (1991) *J. Biol. Chem.* **266,** 7345–7352
47. Kamata, T., Ambo, H., Puzon-McLaughlin, W., Tieu, K. K., Handa, M., Ikeda, Y., and Takada, Y. (2004) *Biochem. J.* **378,** 1079–1082
48. Calzada, M. J., Alvarez, M. V., and Gonzalez-Rodriguez, J. (2002) *J. Biol. Chem.* **277,** 39899–39908
49. Frelinger, A. L., III, Lam, S. C., Plow, E. F., Smith, M. A., Loftus, J. C., and Ginsberg, M. H. (1988) *J. Biol. Chem.* **263,** 12397–12402
50. Takagi, J., Strokovich, K., Springer, T. A., and Walz, T. (2003) *EMBO J.* **22,** 4607–4615
51. Yauch, R. L., Kazarov, A. R., Desai, B., Lee, R. T., and Hemler, M. E. (2000) *J. Biol. Chem.* **275,** 9230–9238
52. Borges, E., Jan, Y., and Ruoslahti, E. (2000) *J. Biol. Chem.* **275,** 39867–39873
53. Selheim, F., Holmsen, H., and Vassbotn, F. S. (2002) *FEBS Lett.* **512,** 107–110
54. Fujimoto, T. T., Katsutani, S., Shimomura, T., and Fujimura, K. (2003) *J. Biol. Chem.* **278,** 26655–26665

Critical cysteine residues for regulation of integrin αIIbβ3 are clustered in the epidermal growth factor domains of the β3 subunit

Tetsuji KAMATA*, Hironobu AMBO†, Wilma PUZON-McLAUGHLIN*, Kenneth Khiem TIEU*, Makoto HANDA†, Yasuo IKEDA† and Yoshikazu TAKADA*[1]

*Department of Cell Biology, The Scripps Research Institute, 10550 N. Torrey Pines Road, La Jolla, CA 92037, U.S.A., †Department of Internal Medicine, Keio University School of Medicine, Shinano-machi, Shinjuku, Tokyo, Japan

Chemical or enzymic reduction/oxidation of integrin cysteine residues (e.g. by reducing agents and protein disulphide isomerase) may be a mechanism for regulating integrin function. It has also been proposed that unique cysteine residues in the integrin β3 subunit are involved in the regulation of αIIbβ3. In the present study, we studied systematically the role of disulphide bonds in β3 on the ligand-binding function of αIIbβ3 by mutating individual cysteine residues of β3 to serine. We found that the disulphide bonds that are critical for αIIbβ3 regulation are clustered within the EGF (epidermal growth factor) domains. Interestingly, disrupting only a single disulphide bond in the EGF domains was enough to activate αIIbβ3 fully. In contrast, only two (of 13) disulphide bonds tested outside the EGF domains activated αIIbβ3. These results suggest that the disulphide bonds in the EGF domains should be intact to keep αIIbβ3 in an inactive state, and that there is no unique cysteine residue in the EGF domain critical for regulating the receptor. The cysteine residues in the EGF domains are potential targets for chemical or enzymic reduction.

Key words: αIIβ3 integrin, disulphide bond, epidermal growth factor domain (EGF domain), fibrinogen, integrin activation, mutagenesis.

INTRODUCTION

Integrins are a family of cell-adhesion receptors that mediate cell–extracellular matrix interactions and cell–cell interactions [1]. It has been proposed that signalling from inside the cells regulates the ligand-binding affinity of integrins by designated inside-out signalling (reviewed in [2]). It has also been proposed that integrins may be regulated by chemical and enzymic oxidation/reduction (e.g. by dithiothreitol, NO or protein disulphide isomerase). Integrin αIIbβ3 (glycoprotein IIb–IIIa, CD41/CD61), a platelet fibrinogen receptor, plays a critical role in primary haemostasis by mediating interactions between platelets and fibrinogen [3]. It has been reported that dithiothreitol induces specific binding of purified αIIbβ3 to fibrinogen, and exposes a ligand-induced binding site (LIBS) on both αIIb and β3 [4]. These effects appear to be the result of a direct action of dithiothreitol on αIIbβ3. It has been reported that the redox potential of blood regulates the activation of αIIbβ3 and that disulphide bond cleavage with sulphydryl generation in β3 is involved in activation of this receptor [5]. Thus evidence is accumulating that reduction/oxidation of disulphide linkages may regulate αIIbβ3.

The crystal structure of αvβ3, another fibrinogen receptor with the common β3 subunit, shows that the β3 subunit has at least two EGF (epidermal growth factor)-like domains (EGF-3 and -4) and probably has two additional EGF domains (EGF-1 and -2) at the stalk region of β3 [6]. The β3 subunit contains 56 cysteine residues that are highly conserved among β subunits and that are involved in disulphide bond formation [7]. It has recently been shown that there is a difference in conformation between the active and inactive forms of integrin αIIbβ3 [8], which may come from the difference in the number and positions of unpaired cysteine residues [9]. It has been proposed that a select group of unpaired cysteine residues exhibit the properties of a redox site involved in integrin activation. In a recent model [10], the conformational transition from resting to active integrin proceeds through a series of changes in the position and number of disulphide bonds; the positions of the cysteine residues involved in this process have not been clearly defined.

It has been reported that the natural $Cys^{598} \rightarrow$ Tyr mutation [11] and the $Cys^{560} \rightarrow$ Arg mutation [12] of the β3 subunit activates αIIbβ3. Also disrupting the Cys^{435}–Cys^{5} disulphide bond [13], or disrupting the Cys^{663}–Cys^{687} disulphide bond [14] constitutively activates αIIbβ3. It has also been reported that disruption of a disulphide bond between Cys^{406} and Cys^{655} does not affect αIIbβ3 ligand binding [15]. It has not been established, however, whether or not the effect of disrupted disulphide bonds is specific to their positions.

In the present paper, we tested systematically the role of disulphide bonds in β3 in the regulation of αIIbβ3 by mutating individual cysteine residues (29 in total). We found that the cysteine mutations that activate αIIbβ3 are clustered within the EGF domains of β3. In contrast, mutating cysteine residues outside the EGF domains did not activate αIIbβ3, with few exceptions. These results suggest that disulphide bonds in the EGF domains may be critically involved in integrin regulation and are potential targets for chemical or enzymic reduction.

EXPERIMENTAL

Monoclonal antibodies (mAbs)

PL98DF6 [16] was from Dr J. Ylänne (Biocenter Oulu and Department of Biochemistry, University of Oulu, Oulu, Finland). PT25-2 was generated as described previously [17].

Abbreviations used: CHO, Chinese-hamster ovary; DMEM, Dulbecco's modified Eagle's medium; EGF, epidermal growth factor; mAb, monoclonal antibody; PE, phycoerythrin.

[1] To whom correspondence should be addressed, at the present address: Department of Dermatology, University of California at Davis Medical Center, Research III, Suite 3300, 4645 2nd Avenue, Sacramento, CA 95817, U.S.A. (e-mail ytakada@ucdavis.edu).

Construction and transfection of cDNAs for human β3 mutants

Wild-type human β3 cDNA was subcloned into pBJ-1 vector, and mutation was introduced [18]. The presence of mutation was verified by DNA sequencing. Wild-type and mutant β3 cDNA constructs in pBJ-1 vector (20 μg) were transfected by electroporation into CHO (Chinese-hamster ovary) cells (1×10^7 cells) [19], together with wild-type αIIb in pBJ-1 vector. Transfected cells were maintained in DMEM (Dulbecco's modified Eagle's medium), supplemented with 10% (v/v) foetal calf serum at 37 °C in 6% CO_2 for 2 days. Then the cells were detached with 3.5 mM EDTA and used for assays.

Flow cytometry

Cells were washed once with DMEM and were then resuspended in the same medium. Cell suspension (50 μl) was incubated with an equal volume of primary mAb (1:250 dilution of ascites or 10 μg/ml of purified mAb) on ice for 30 min. After washing with DMEM, cells were incubated with FITC-conjugated anti-mouse IgG (Biosource, Camarillo, CA, U.S.A.) for 30 min on ice.

Fibrinogen binding

Human fibrinogen (Enzyme Research Laboratories, South Bend, IN, U.S.A.) was labelled with FITC as described previously [20,21]. Fibrinogen binding to cells transiently expressing αIIbβ3 was determined as described previously in [22] with some modifications. Briefly, cells were first incubated with PL98DF6 followed by phycoerythrin (PE)-conjugated anti-mouse IgG (Biosource). Cells were washed with modified Tyrode–Hepes buffer (5 mM Hepes, 5 mM glucose, 0.2 mg/ml BSA and 1× Tyrode solution), pH 7.4, supplemented with 2 mM $CaCl_2$ and 2 mM $MgCl_2$. Cells were then incubated with 150 μg/ml FITC-labelled fibrinogen in the presence of 10 μg/ml control mouse IgG or PT25-2 in the same buffer for 30 min. After removing unbound fibrinogen, cells were resuspended in Hepes-buffered saline, pH 7.4, supplemented with 2 mM $CaCl_2$ and 2 mM $MgCl_2$. Binding of fibrinogen (FITC staining) was analysed on a gated subset of cells highly positive for αIIbβ3 expression (PE staining) in FACScan. Relative fibrinogen binding was calculated as $(F_{PT} - F_{mIgG})/(Fw_{PT} - Fw_{mIgG})$, where F_{PT} is the median fluorescence intensity of fibrinogen binding in the presence of PT25-2, F_{mIgG} is the median fluorescence intensity of fibrinogen binding in the presence of normal mouse IgG, Fw_{PT} is the median fluorescence intensity of fibrinogen binding to cells expressing wild-type αIIbβ3 in the presence of PT25-2, and Fw_{mIgG} is the median fluorescence intensity of fibrinogen binding to cells expressing wild-type αIIbβ3 in the presence of normal mouse IgG. Relative αIIbβ3 expression is a ratio of the median fluorescence intensity of PL98DF6 binding to the gated population to the median fluorescence intensity of PL98DF6 binding to the gated population expressing wild-type αIIbβ3. The activation index was calculated as $100 \times (F_o - F_r)/(F_o\ PT - F_r\ PT)$, where F_o is the median fluorescence intensity of fibrinogen binding, F_r is the median fluorescent intensity of fibrinogen binding in the presence of 1 mM GRGDS peptide [22,23], F_o PT is the median fluorescence intensity of fibrinogen binding in the presence of 10 μg/ml PT25-2, and F_r PT is the median fluorescence intensity of fibrinogen binding in the presence of 10 μg/ml PT25-2 and GRGDS peptide.

RESULTS AND DISCUSSION

We reported previously that the $Cys^{560} \rightarrow$ Phe mutation in the EGF domains of β3 [24] is associated with the bleeding tendency in

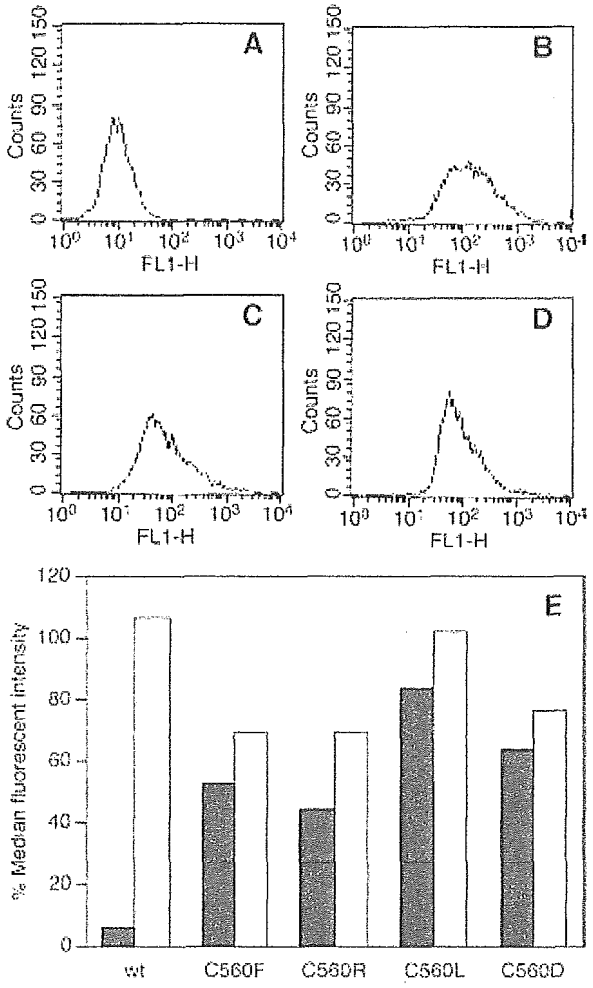

Figure 1 Effects of the β3 $Cys^{560} \rightarrow$ Phe mutation on binding of soluble fibrinogen to αIIbβ3 (A–D) and effects of mutating Cys^{560} to other amino acid residues on the activation status of αIIbβ3 (E)

CHO cells transiently expressing wild-type (**A**, **B**) or the $C^{560} \rightarrow$ Phe mutant (**C**, **D**) of αIIbβ3 were stained with PL98DF6 (anti-αIIb mAb), followed by PE-conjugated anti-mouse IgG. After washing, cells were incubated with FITC–fibrinogen in the presence of control mouse IgG (**A**, **C**) or activating mAb PT25-2 (**B**, **D**). The solid histograms represent FITC-fibrinogen binding (FL1) to αIIbβ3-positive cells (FL2 > 100). The blank histograms represent FITC-fibrinogen binding in the presence of 1 mM GRGDS peptide. (**E**) The effects of mutating Cys^{560} to several other amino acid residues on the activation status of αIIbβ3. Wild-type (wt) or mutant (one-letter amino acid codes are used) β3 was transiently transfected together with wild-type αIIb into CHO cells. FITC–fibrinogen binding to αIIbβ3-positive cells was examined in the presence of PT25-2 (open bars) and of control mouse IgG (closed bars). Mutating Cys^{560} to glycine, alanine, serine methionine, arginine, asparagine, tyrosine, tryptophan and histidine also constitutively activated αIIbβ3 (results not shown).

Glanzmann's thrombasthenia. It has been reported that the similar $Cys^{560} \rightarrow$ Arg mutation activates αIIbβ3 [12]. To study the effect of the $Cys^{560} \rightarrow$ Phe mutation on αIIbβ3 function, we transiently expressed the mutant on the surface of CHO cells together with wild-type αIIb. We examined the ability of the αIIb/β3 $Cys^{560} \rightarrow$ Phe mutant to bind to soluble FITC-labelled fibrinogen with or without an anti-αIIbβ3 mAb PT25-2, which specifically activates αIIbβ3. Wild-type αIIbβ3 in CHO cells does not bind to ligand unless it is activated [19,25]. We selected cells that express wild-type or mutant αIIbβ3 at high levels, and tested their ability to bind to soluble fibrinogen. The αIIb/β3 $Cys^{560} \rightarrow$ Phe mutant bound to soluble fibrinogen without activation (Figures 1A–1D), suggesting that the mutation induced constitutive activation of

Cys^{23}–$Cys^{[illegible]}$, Cys^{29}–$Cys^{[illegible]}$, Cys^{49}–$Cys^{[illegible]}$, Cys^{177}–Cys^{184},
Cys^{232}–$Cys^{[illegible]}$, Cys^{454}–$Cys^{[illegible]}$, Cys^{466}–$Cys^{[illegible]}$, Cys^{435}–$Cys^{[illegible]}$,
Cys^{435}–$Cys^{[illegible]}$,

Cys^{460}–Cys^{471}, Cys^{462}–Cys^{487}, Cys^{473}–Cys^{486}, Cys^{495}–Cys^{503},
Cys^{508}–Cys^{521}, Cys^{523}–Cys^{528}, Cys^{536}–Cys^{544}, Cys^{542}–Cys^{547},
Cys^{549}–Cys^{558}, Cys^{560}–Cys^{583}, Cys^{575}–Cys^{586}, Cys^{581}–Cys^{567},
Cys^{588}–Cys^{598}, Cys^{601}–Cys^{604},

Cys^{633}–$Cys^{[illegible]}$, Cys^{635}–$Cys^{[illegible]}$, Cys^{687}–$Cys^{[illegible]}$

Figure 2 β3 disulphide bonds tested in the present study

The assignments of the disulphide bonds are based on the crystal structure of αvβ3 [6]. The grey shaded area indicates the EGF domain. The cysteine residues in bold were mutated to serine.

αIIbβ3. GRGDS peptide (Figures 1A–1D), and function-blocking anti-αIIbβ3 mAb, completely blocked fibrinogen binding to the αIIb/β3 Cys^{560} → Phe mutant (results not shown), suggesting that this binding is specific to αIIbβ3. To test whether this constitutive activation is specific to the Cys^{560} → Phe mutation, we mutated Cys^{560} to 12 different amino acids (serine, glycine, leucine, alanine, methionine, aspartic acid, arginine, asparagine, tyrosine, histidine, tryptophan and phenylalanine). All of these mutants constitutively activated αIIbβ3 (Figure 1E). These results suggest that the constitutive activation of αIIbβ3 by the Cys^{560} → Phe (and probably the Cys^{560} → Arg) mutation is not unique to the Cys^{560} → Phe mutation, and that disruption of the disulphide bond is primarily responsible for the constitutive activation of αIIbβ3.

We studied the role of other disulphide bonds in the β3 subunit in regulating ligand binding to αIIbβ3. To do this we mutated the individual cysteine residues of β3 to serine to disrupt individual disulphide bonds according to the assignments of disulphide bonds based on the αvβ3 crystal structure (Figure 2). We transiently expressed the β3 mutants together with wild-type αIIb in CHO cells and tested their ability to bind to soluble fibrinogen as described above. We found that mutating the cysteine residues at positions 435, 460, 462, 473, 495, 508, 521, 523, 536, 542, 549, 560, 575, 581, 588, 601 and 687 induced the binding of soluble fibrinogen to αIIbβ3 without activating mAb PT25-2 (Figure 3A). The anti-αIIbβ3 activating mAb PT25-2 had only a minor effect on fibrinogen binding to constitutively active mutants. This suggests that these mutations constitutively activate αIIbβ3 (with high activation indexes) (Figure 3B). Interestingly, these cysteine residues are clustered within the EGF domains (15 out of 17). These results also suggest that disruption of a single disulphide bond within the EGF domains may lead to constitutive activation of αIIbβ3.

In contrast, we found that mutating the cysteine residues at positions 23, 26, 49, 374, 406, 433, 631 and 635 did not significantly activate αIIbβ3 (with low activation indexes). These β3 mutants bound to soluble fibrinogen similarly to wild-type in the presence of mAb PT25-2, indicating that their ligand-binding functions were intact. These cysteine residues are all located outside the EGF domains. The C^{171} → Ser and C^{184} → Ser mutants did not bind to fibrinogen even when activated with mAb PT25-2, suggesting that mutating Cys^{171} and Cys^{184} inactivated αIIbβ3. A likely reason for this is that these residues are located in the putative fibrinogen-binding sites [26,27].

The present study suggests that the C^{560} → Phe mutation of β3 [24] activates αIIbβ3, like the C^{560} → Arg mutation [12],

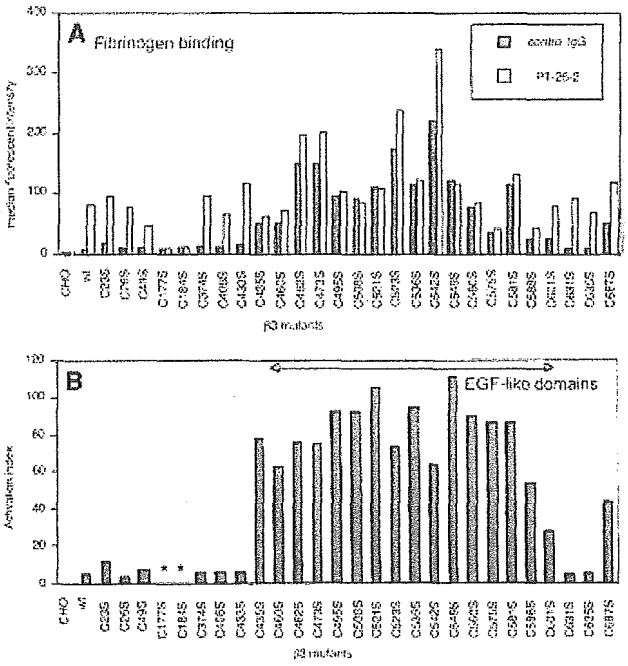

Figure 3 Effects of mutating individual cysteine residues on the activation status of αIIbβ3

Individual β3 cysteine residues were mutated to serine to disrupt disulphide bonds according to the disulphide bond assignment based on the crystal structure of αvβ3 [6] as shown in Figure 2. Individual β3 mutants (one-letter amino acid codes are used) were expressed on CHO cells together with wild-type (wt) αIIb as described above. The ability of αIIbβ3-positive cells to bind to soluble fibrinogen was measured in the presence and absence of activating anti-αIIbβ3 mAb PT25-2 (**A**), and the activation index was calculated (**B**). The Cys^{177} → Ser and Cys^{184} → Ser mutants were inactive (shown by *). The Cys^{233} → Ser and Cys^{273} → Ser mutants were not tested due to poor expression.

and this activation does not depend on the amino acid species to which the cysteine residue is mutated, since mutating Cys^{560} to twelve other different amino acid residues generates the same effects. It is likely that the activation is due to disruption of the disulphide linkage. It has been reported that another natural mutation of a cysteine residue (Cys^{598} → Tyr) [11], disrupting the Cys^{435}–Cys^{5} disulphide bond [13] or disrupting the Cys^{663}–Cys^{687} disulphide bond [14], constitutively activates αIIbβ3. It has been reported that disruption of a disulphide bond between Cys^{406} and Cys^{655} does not affect αIIbβ3 ligand binding [15]. It has not been established, however, whether the effect of disrupting disulphide bonds is specific to their positions. We thus mutated systematically individual cysteine residues of β3 and studied their effects on the ligand-binding function of αIIbβ3. The present results are consistent with the previous reports [11,13–15], and expanded the previous findings further. We have shown that the cysteine residue mutations that activate αIIbβ3 are clustered within the EGF domains. Mutating cysteine residues outside the EGF domains did not induce activation of αIIbβ3, with few exceptions. These results suggest that disulphide bonds in the EGF domains keep αIIbβ3 in an inactive form, and disruption of a single disulphide bond in the EGF domain is enough to induce activation of αIIbβ3. It is suggested that disulphide bonds in the EGF domains should be completely intact when αIIbβ3 is inactive.

It has been proposed that the integrin proceeds through a series of changes in the position and number of disulphide bonds (redox transition) [10]. The positions of unpaired cysteine residues (redox sites) have not been reported, but several cysteine residues in the cysteine-rich EGF domains (at positions 655, 457

and 495) are likely candidates [10]. The results in the present study do not fit well with this model, since the present results suggest that the unpaired cysteine residues cannot be present in the EGF domains of $\beta 3$ when the receptor is inactive. Interestingly, there is no unique cysteine residue that is critical for regulation of the integrin in the EGF domains. The present study, however, suggests that the inactive form might have unpaired cysteine residues outside the EGF domains. There are several cysteine residues, the mutation of which does not affect fibrinogen binding (positions 23, 26, 49, 374, 406, 433, 631 and 635), that could be unpaired in an inactive form of αIIb$\beta 3$. Further biochemical studies will be required to test whether the cysteine residues outside the EGF domain of $\beta 3$ are involved in regulation of the integrin.

The $\alpha v\beta 3$ crystal structure is sharply bent at the stalk region, and it has been proposed that the EGF-3 and -4 domains (and probably the EGF-1 and -2 domains) generate a rigid rod-like module [6]. It has been proposed that the bent form is inactive and the extended form is active [28]. Interestingly the αv stalk region contains three β-sandwich domains, thigh and calf-1 and -2 domains [6], and the two calf domains generate a rigid entity (the calf module) at the C-terminal side of the stalk. Although the disulphide bonds in the EGF domains should be intact when the integrin is in an inactive form, it is unclear how disruption of disulphide bonds in the EGF domains makes the integrin active. It would be interesting to test whether the integrins are bent or extended when one of the disulphide bonds of $\beta 3$ is disrupted.

We thank J. Ylänne for providing valuable reagents. This work is supported by the NIH (National Institutes of Health) grant GM47157 (to Y.T.) and the US Army DAMD17-97-1-7105 grant (to T.K.).

REFERENCES

1 Hynes, R. O. (1992) Integrins: versatility, modulation and signaling in cell adhesion. Cell **69**, 11–25
2 Shattil, S. J., Kashiwagi, H. and Pampori, N. (1998) Integrin signaling: the platelet paradigm. Blood **91**, 2645–2657
3 Phillips, D. R., Charo, I. F., Parise, L. V. and Fitzgerald, L. A. (1988) The platelet membrane glycoprotein IIb–IIIa complex. Blood **71**, 831–843
4 Kouns, W., Steiner, B., Kunicki, T., Moog, S., Jutzi, J., Jennings, L., Cazenave, J. and Lanza, F. (1994) Activation of the fibrinogen binding site on platelets isolated from a patient with the Strasbourg I variant of Glanzmann's thrombasthenia. Blood **84**, 1108–1115
5 Essex, D. W. and Li, M. (2003) Redox control of platelet aggregation. Biochemistry **42**, 129–136
6 Xiong, J.-P., Stehle, T., Diefenbach, B., Zhang, R., Dunker, R., Scott, D. L., Andrzej, J., Goodman, S. L. and Arnaout, M. A. (2001) Crystal structure of the extracellular segment of integrin $\alpha v\beta 3$. Science **294**, 339–345
7 Calvete, J. J., Henschen, A. and Gonzalez-Rodriguez, J. (1991) Assignment of disulphide bonds in human platelet GPIIIa. Biochem. J. **274**, 63–71
8 Yan, B., Hu, D. D., Knowles, S. K. and Smith, J. W. (2000) Probing chemical and conformational differences in the resting and active conformers of platelet integrin αIIb$\beta 3$. J. Biol. Chem. **275**, 7249–7260
9 Yan, B. and Smith, J. W. (2000) A redox site involved in integrin activation. J. Biol. Chem. **275**, 39964–39972
10 Yan, B. and Smith, J. W. (2001) Mechanism of integrin activation by disulfide bond reduction. Biochemistry **40**, 8861–8867
11 Chen, P., Melchior, C., Brons, N. H., Schlegel, N., Caen, J. and Kieffer, N. (2001) Probing conformational changes in the I-like domain and the cysteine-rich repeat of human $\beta 3$ integrins following disulfide bond disruption by cysteine mutations: identification of cysteine 598 involved in αIIb$\beta 3$ activation. J. Biol. Chem. **276**, 38628–38635
12 Ruiz, C., Liu, C. Y., Sun, Q. H., Sigaud-Fiks, M., Fressinaud, E., Muller, J. Y., Nurden, P., Nurden, A. T., Newman, P. J. and Valentin, N. (2001) A point mutation in the cysteine-rich domain of glycoprotein (GP) IIIa results in the expression of a GPIIb–IIIa (αIIb$\beta 3$) integrin receptor locked in a high-affinity state and a Glanzmann thrombasthenia-like phenotype. Blood **98**, 2432–2441
13 Sun, Q. H., Liu, C. Y., Wang, R., Paddock, C. and Newman, P. J. (2002) Disruption of the long-range GPIIIa Cys^5-Cys^{435} disulfide bond results in the production of constitutively active GPIIb–IIIa (αIIb$\beta 3$) integrin complexes. Blood **100**, 2094–2101
14 Butta, N., Arias-Salgado, E. G., Gonzalez-Manchon, C., Ferrer, M., Larrucea, S., Ayuso, M. S. and Parrilla, R. (2003) Disruption of the $\beta 3$ 663–687 disulfide bridge confers constitutive activity to $\beta 3$ integrins. Blood **102**, 2491–2497
15 Wang, R., Peterson, J., Aster, R. H. and Newman, P. J. (1997) Disruption of a long-range disulfide bond between residues Cys^{406} and Cys^{655} in glycoprotein IIIa does not affect the function of platelet glycoprotein IIb–IIIa. Blood **90**, 1718–1719
16 Ylanne, J., Hormia, M., Jarvinen, M., Vartio, T. and Virtanen, I. (1988) Platelet glycoprotein IIb/IIIa complex in cultured cells: localization in focal adhesion sites in spreading HEL cells. Blood **72**, 1478–1486
17 Tokuhira, M., Handa, M., Kamata, T., Oda, A., Katayama, M., Tomiyama, Y., Murata, M., Kawai, Y., Watanabe, K. and Ikeda, Y. (1996) A novel regulatory epitope defined by a murine monoclonal antibody to the platelet GPIIb–IIIa complex (αIIb$\beta 3$ integrin). Thromb. Haemostasis **76**, 1038–1046
18 Deng, W. P. and Nickoloff, J. A. (1992) Site-directed mutagenesis of virtually any plasmid by eliminating a unique site. Anal. Biochem. **200**, 81–88
19 Kamata, T., Irie, A. and Takada, Y. (1996) Critical residues of the αIIb subunit of integrin αIIb$\beta 3$ (GPIIb–IIIa) for binding to fibrinogen and ligand-mimetic antibodies (PAC-1, OP-G2 and LJ-CP3). J. Biol. Chem. **271**, 18610–18615
20 Xia, Z., Wong, T., Liu, Q., Kasirer-Friede, A., Brown, E. and Frojmovic, M. M. (1996) Optimally functional fluorescein isothiocyanate-labelled fibrinogen for quantitative studies of binding to activated platelets and platelet aggregation. Br. J. Haematol. **93**, 204–214
21 Goto, S., Salomon, D. R., Ikeda, Y. and Ruggeri, Z. M. (1995) Characterization of the unique mechanism mediating the shear dependent binding of soluble von Willebrand factor to platelets. J. Biol. Chem. **270**, 23352–23361
22 Hughes, P., O'Toole, T., Ylanne, J., Shattil, S. and Ginsberg, M. (1995) The conserved membrane-proximal region of an integrin cytoplasmic domain specifies ligand binding affinity. J. Biol. Chem. **270**, 12411–12417
23 Hughes, P. E., Shipley, T., O'Toole, T. E. and Shattil, S. (1994) The membrane-proximal region in the $\beta 3$ cytoplasmic domain of integrin αIIb$\beta 3$ plays a key role in affinity modulation. Mol. Biol. Cell **5**, 183a
24 Ambo, H., Kamata, T., Handa, M., Taki, M., Kuwajima, M., Kawai, Y., Oda, A., Murata, M., Takada, Y., Watanabe, K. and Ikeda, Y. (1998) Three novel integrin $\beta 3$ subunit missense mutations (H280P, C560F, and G579S) in thrombasthenia, including one (H280P) prevalent in Japanese patients. Biochem. Biophys. Res. Commun. **251**, 763–768
25 O'Toole, T., Loftus, J., Du, X., Glass, A., Ruggeri, Z., Shattil, S., Plow, E. and Ginsberg, M. (1990) Affinity modulation of the αIIb$\beta 3$ integrin (platelet GPIIb–IIIa) is an intrinsic property of the receptor. Cell Regul. **1**, 883–893
26 Takagi, J., Kamata, T., Meredith, J., Puzon-McLaughlin, W. and Takada, Y. (1997) Changing ligand specificities of $\alpha v\beta 1$ and $\alpha v\beta 3$ integrins by swapping a short diverse sequence of the β subunit. J. Biol. Chem. **272**, 19794–19800
27 Puzon-McLaughlin, W., Kamata, T. and Takada, Y. (2000) Multiple discontinuous ligand-mimetic antibody binding sites define a ligand binding sites in integrin αIIb$\beta 3$. J. Biol. Chem. **275**, 7795–7802
28 Takagi, J. and Springer, T. A. (2002) Integrin activation and structural rearrangement. Immunol. Rev. **186**, 141–163

Received 6 November 2003; accepted 22 December 2003
Published as BJ Immediate Publication 22 December 2003, DOI 10.1042/BJ20031701

Revised Manuscript for J. Artificial Organs

New Strategy of Platelet Substitutes for Enhancing Platelet Aggregation at High Shear Rates; Cooperative Effects of a Mixed System of Fibrinogen γ-Chain Dodecapeptide- or Glycoprotein Ibα-Conjugated Latex Beads under Flow Conditions

Yosuke Okamura, PhD[1), 2)], Makoto Handa, MD, PhD[2)], Hidenori Suzuki, PhD[3)], Yasuo Ikeda, MD, PhD[4)] and Shinji Takeoka, PhD[1)*]

(Received:)

1) Graduate School of Science and Engineering, Waseda University, Tokyo, 169-8555, Japan. 2) Department of Transfusion Medicine & Cell Therapy, School of Medicine, Keio University, Tokyo, 160-8582. 3) Center for Electron Microscopy, the Tokyo Metropolitan Institute of Medical Science, Tokyo, 113-8613. 4) Department of Internal Medicine, School of Medicine, Keio University, Tokyo, 160-8582.

* To whom correspondence should be addressed.
e-mail: takeoka@waseda.jp, Tel: +813-5286-3217, Fax: +813-5286-3217

Key words: platelet substitute, fibrinogen γ-chain dodecapeptide, platelet glycoprotein (GP) Ibα, thrombocytopenia-imitation blood, shear rate

Field: Others

ABSTRACT

In order to construct platelet substitutes that have hemostatic property at a wide range of shear rates, we used on a fibrinogen γ-chain carboxy-terminal sequence; HHLGGAKQAGDV (H12), which recognized the activated platelets at low shear rates, and a recombinant water-soluble moiety of the platelet glycoprotein (rGPIbα), which recognizes von Willebrand factor at high shear rates. Three kinds of samples were prepared for this purpose: H12-conjugated latex beads (H12-latex beads), rGPIbα-latex beads, and H12/rGPIbα-latex beads and evaluated in thrombocytopenia-imitation blood at the various flowing conditions. Based on ADP-induced platelet aggregation studies, the H12-latex beads significantly enhanced platelet aggregation via H12 binding with GPIIb/IIIa activated on the surface of activated platelets, whereas the rGPIbα-latex beads did not support platelet aggregation. In the case of the H12/rGPIbα-latex beads, the function of H12 was suppressed by the steric hindrance of the larger rGPIbα bound to the latex bead. The mixture of the H12-latex beads and the rGPIbα-latex beads adhered to the collagen surface at a wide range of shear rates. In particular, at a high shear rate, a cooperative effect tended to observe in the enhancement of the platelet thrombus formation compared with H12-latex beads or rGPIbα-latex beads alone. We propose that the mixed system of the H12- and rGPIbα-conjugated nanoparticles is a more effective platelet substitute and has enhanced platelet aggregation properties.

INTRODUCTION

Platelet transfusion plays an important role in the supportive therapy of thrombocytopenia caused by cancer or hematologic malignancies, or in the perioperative period. However, the shortage of platelet concentrates has always been a serious issue because of the short storage period (three days in Japan), the insufficient donations, and imbalance of demand and supply. Furthermore, there is the issue of the risk of viral and bacterial infections by transfusion. For these reasons, a number of trials have been conducted to develop platelet substitutes, such as, infusible platelet membranes (IPMs),[1] solubilized platelet membrane protein-conjugated liposomes (Plateletsomes),[2] fibrinogen-bonded red blood cells,[3] fibrinogen-coated albumin microcapsules (Synthocyte),[4] and arginine-glycine-asparaginic acid (RGD) peptide-bound red blood cells (Thromboerythrocytes).[5] However, these platelet substitutes consist of materials derived from blood components.

We also conjugated fibrinogen[6] to biocompatible carriers such as polymerized albumin particles (polyAlb)[7-9] and phospholipid vesicles (liposomes).[10-13] Fibrinogen-conjugates facilitated platelet aggregation on an activated platelet-immobilized surface *in vitro* by the recruitment of flowing platelets in the aggregates after their attachment.[6] However, fibrinogen isolated from human blood tends to precipitate at 4 °C within a few hours.[6] Recently, we have focused on fibrinogen dodecapeptide (HHLGGAKQAGDV; H12)[14-18] and confirmed that the H12-conjugates showed minimal interaction with non-activated platelets[19] and enhanced the

in vitro platelet thrombus formation on the collagen-immobilized plate under the flowing of thrombocytopenia-imitation blood.[9,19] However, this effect was limited to low shear rates (e.g., 150 s^{-1}).

We also developed the water-soluble part of GPIbα as a recombinant product (rGPIbα) as a key recognition site of platelet substitutes.[20-22] In previous studies we found that rGPIbα-polyAlb accumulated on the VWF-immobilized surface at high shear rates (e.g., 1600 s^{-1}),[10] reflecting the interaction of natural GPIbα with VWF.[23-26] Therefore, we consider that H12- or rGPIbα-particles alone would not be effective for the recognition of the sites of vascular injury at a wide range of shear rates.

In this study, we selected H12 and rGPIbα as recognition sites of platelet substitute and prepared four kinds of samples; H12/rGPIbα-latex beads, which conjugated both H12 and rGPIbα to the same latex bead, H12-latex beads, rGPIbα-latex beads, and the mixture of the H12-latex beads and the rGPIbα-latex beads. Latex beads were very useful carriers for *in vitro* studies because of their uniform size and ease of confirmation by microscopic observation.

MATERIALS & METHODS

Reagents

Fibrinogen γ-chain dodecapeptide with an added cysteine to the amino-terminal (H12; C-HHLGGAKQAGDV) was synthesized using a solid-phase synthesizer by BEX (Tokyo, Japan). Latex beads (Polybead™ or Fluoresbrite™, 1 μm diameter) and *N*-succinimidyl 3-(2-pyridyldithio) propionate (SPDP) were purchased from Polysciences (Warrington, PA) and Pierce (Rockford, IL), respectively. An anticoagulant D-Phe-Pro-Arg-chloromethylketone (PPACK) was purchased from Calbiochem (San Diego, CA). 3,3'-Dihexyloxacarbocyanine iodide ($DiOC_6$), which is a platelet fluorescent dye, was purchased from Molecular Probes (Eugene, OR). The monoclonal antibodies against rGPIbα, GUR20-5, and horseradish peroxidase-conjugated GUR83-35 were purchased from Takara Bio (Otsu, Japan). Recombinant human serum albumin (rHSA) and purified rGPIbα were kindly donated by Mitsubishi Pharma (Osaka, Japan).

Preparation of H12- or rGPIbα-conjugated latex beads

Latex beads bearing H12: Latex beads were mixed with an rHSA solution (50 mg/mL) and incubated at room temperature (r.t.) for 2 hr to coat the surface of the latex bead with rHSA. After the separation of the remaining rHSA by centrifugation (13000*g*, 5 min, 4 °C, 3 times), the rHSA-coated latex beads were suspended in phosphate-buffered saline (PBS, pH 7.4). A

solution of SPDP in ethanol (5 mM, 5 μL) was added to the suspension of the latex beads (4.0 x 10^6/μL) and incubated for 30 min at r.t. The unreacted SPDP and the by-products were separated by centrifugation, and the pyridyl disulfide (PD)-bonded rHSA-coated latex beads were collected. The suspension of the latex beads (4.0 x 10^6/μL) was mixed with a solution of H12 (10 mM, 8 μL) and reacted at 25 °C for 12 hr by the thiol-disulfide exchange reaction. The unreacted H12 was removed by centrifugation to purify the latex beads bearing H12 (H12-latex beads, 2.0 x 10^6/μL). The concentration of the H12 conjugated to the latex beads was determined by indirect quantification of the 2-thiopyridone (2TP) that was liberated during a thiol-disulfide exchange reaction using high pressure liquid chromatography (HPLC) on a TSK-GEL G3000SW_{XL} column (7.8 mm o.d. x 300 mm h in PBS at 1 mL/min), by measuring the absorbance of the column flow at 343 nm.

Latex beads bearing rGPIbα: A solution of SPDP in ethanol (5 mM, 5 μL) was added to an rGPIbα solution (4.3 mg/mL, 200 μL) and incubated for 20 min at r.t.. A dithiothreitol solution (final concentration; 20 mM) was added to the PD-rGPIbα solution to obtain SH-rGPIbα after separation with GPC (sephadex G25). The solution of the SH-rGPIbα (1.0 mg/mL) was mixed with a suspension of the PD-bonded rHSA-coated latex beads obtained as described above, and reacted at 25 °C for 12 hr. The unreacted reagents were removed by centrifugation to separate the latex beads bearing rGPIbα (rGPIbα-latex beads, 2.0 x 10^6/μL).

The concentration of the rGPIbα conjugated on the latex bead was determined with a sandwich enzyme-linked immunosorbent assay (ELISA) with GUR 20-5 and horseradish peroxidase-conjugated GUR83-35.[19]

Latex beads bearing both H12 and rGPIbα. A solution of SPDP in ethanol (20 mM, 10 μL) was added to a suspension of rHSA-coated latex beads (4.0 x 10^6 /μL) and incubated for 30 min at r.t. The suspension of the PD-latex beads (4.0 x 10^6 /μL) was mixed with an aqueous solution of H12 (4 mM, 8 μL) and reacted at 25 °C for 12 hr. The unreacted reagents were removed by centrifugation and the purified H12-latex beads (2.0 x 10^6 /μL) were obtained. One or two mL of a SH-rGPIbα solution (1.0 mg/mL) was added to the dispersion of the H12-latex beads, and incubated for 12 hr at r.t. The latex beads bearing both H12 and rGPIbα (H12/rGPIbα-latex beads) were purified by centrifugation. The concentration of H12 or rGPIbα conjugated on the latex bead was determined by HPLC or a sandwich ELISA, respectively, as described above.

Platelet aggregation study

Blood withdrawn from healthy volunteers was mixed with 10% volume of 3.8% (w/v) sodium citrate. Platelet-rich plasma (PRP) was prepared by centrifugation (100*g*, 15 min, 22 °C), and the platelet concentration of PRP was adjusted to 2.0 x 10^5 /μL by platelet-poor